Journal of Applied Polymer Science

Immobilized Pd metal-complex on polymeric resin with high surface areas for recyclable catalyst: Effect of the immobilization method on nature of palladium species.

--Manuscript Draft--

Full Title:	Immobilized Pd metal-complex on polymeric resin with high surface areas for recyclable catalyst: Effect of the immobilization method on nature of palladium species.
Manuscript Number:	app.20222758R1
Article Type:	Research Article
Corresponding Author:	Claudio Mella, Ph.D Universidad de Concepción Concepcion, biobio CHILE
Corresponding Author E-Mail:	claudiomella@udec.cl
Corresponding Author's Institution:	Universidad de Concepción
Order of Authors:	Claudio Mella
	Gina Pecchi
	Cyril Godard, PhD
	Carmen Claver
	Abdiel Márquez
	Cristian H Campos
Manuscript Classifications:	Catalysts; Resins; Spectroscopy; Synthesis and Processing Techniques
Additional Information:	
Question	**Response**
Please provide the principal investigator's name and affiliation. (Principal investigator MUST be listed as a co-author on the submission; please DO NOT list all other co-authors in this section.)	Claudio Mella, Facultad de Ciencias Químicas, Universidad de Concepción, Casilla Concepción 160-C, Chile
Please submit a plain text version of your cover letter here. If you also wish to upload a file containing your cover letter, please note it here and upload the file when prompted to upload manuscript files. Please note, if you are submitting a revision of your manuscript, there is an opportunity for you to provide your responses to the reviewers later; please do not add them to the cover letter.	Dear Editor, Dr. Stefan Spiegel Please find enclosed the manuscript entitled “Immobilized Pd metal-complex on high surface polymers for recyclable catalyst: Effect of the immobilization method on nature of palladium species.” by Claudio Mella, Gina Pecchi, Cyril Godard, Carmen Claver, Abdiel Marque, Javiera Herrera and Cristian H Campos, to be considered for publishing as an original paper in the Journal of applied polymer science. It is known that immobilization or heterogenization of the metal complex is an interesting route to obtaining recyclable catalysts, for this polymer’s materials, have great advantages allowing different methodological procedures for metal complex immobilization. However, is important to clarify the better methodological approach to obtain a well-defined catalyst supported for Palladium-salophen type metal complex over crosslinked polymer matrix with a large surface area. This manuscript is based on proving two approaches reported for immobilization of coordination compounds, looking to get the same metal complex supported on a polymeric surface. The target is to obtain a well-distributed metal complex to apply as a heterogeneous catalyst on heck coupling reaction, special interest was centered on

	characterization of catalytic species present on the larger surface polymer by spectroscopical characterization, where XPS is the powerfull tools to discriminate between both approaches. Additionally, the mechanical and thermal properties of the hydrogels were described, as well as their catalytic performance and reusability. The results suggest that Palladium metal complexes can be obtained only by one approach, while the second one produces a mixture between metal nanoparticles and palladium acetate, used as the metal precursor of catalyst synthesis. Each catalyst was evaluated on the Heck coupling of methyl acrylate and iodobenzene, showing important differences in metal leaching behavior and catalytic performance. Additionally, the reusability of a better catalyst was evaluated over four cycles with a minor decrease of activity. This contribution has not been previously, either simultaneously, submitted to this or another journal. This submission was completed with all requirements established by the journal of applied polymer science and is in compliance with the code of conduct and conflict of interest as described in the Guide for Authors. Besides, the references are in the correct format and the manuscript is in the correct order upon submission. Thank you for your consideration. Sincerely yours, Claudio Mella Postdoctoral research, Universidad de Concepción Concepcion, Chile
Author Comments:	Dear Editor, We are pleased to submit the revised version of the manuscript entitled “Immobilized Pd metal-complex on polymeric resin with high surface areas for recyclable catalyst: Effect of the immobilization method on nature of palladium species” to be considered for publication in the Journal of Applied Polymer Science. We sincerely thank to you and the reviewers for their valuable and constructive comments and corrections to our manuscript. The authors have carefully considered the comments and tried our best to address every one of them. The authors welcome further constructive comments if any. We have modified it accordingly, and the answers/comments are listed in detail herein, point by point. Finally, the corrections were marked in yellow in this revised version of the manuscript.
Response to Reviewers:	Dear Reviewer, We sincerely thank to you for your valuable and constructive comments and corrections to our manuscript. We have modified it accordingly, and the answers/comments are listed in detail herein, point by point: Reviewer #1: In the manuscript entitled "Immobilized Pd metal-complex on polymeric resin with high surface areas for recyclable catalyst: Effect of the immobilization method on nature of palladium species.", C. Mella et al. report a one-pot synthetic method and a multi-step for pseudo-homogeneous Palladium-based catalyst. In their methods, the palladium-coordinated monomers were converted to the catalytic polymer that can reuse and easily separated from the reaction mixture. Although the polymerization strategy using palladium coordinated monomers as a synthetic approach of supporting resin is novel, however, there are several major concerns regarding the catalytic efficiency of their palladium-encapsulated resins and the unclear scientific or technical advances. Thus, as long as the authors address the following issues, I do not have the enthusiasm to support its publication in Journal of Applied Polymer Science.

Major issues 1.
Considering their concept to fabricate a pseudo-homogeneous catalyst that has both reusability and improved catalytic activity compared to heterogeneous catalysts, the authors should demonstrate that the catalysts possess improved catalytic activity than the heterogeneous catalysts. Since palladium is located not only on the surface of the resin but also inside the resin, the catalyst activity is inevitably lost compared to homogeneous catalysts due to the diffusion problem of the reactants entering the resin. Thus, the main goal of fabricating a pseudo-homogeneous is to minimize the loss of activity and maximize reusability. Reusability was demonstrated in the manuscript. But they also need to show how much the activity was reduced compared to the same amount of homogenous catalysts and how their method minimized the decrease in catalytic activity.

Answer: Sincerely grateful for the comments. In the revised version of the manuscript, we provided information comparing the our catalyst with the usually reported homogeneous catalyst (PdCH3COO)2).

Major issues 2
The resin size might affect the activity of pseudo-homogeneous catalysts. So, if possible, the author needed to optimize the size of the resin.

Answer: Sincerely grateful for the comments; the study to optimize the size of resins was carried out previously in the context of Claudio Mella's doctoral thesis. The results demonstrate that different continuous phase/ discontinuous phase ratios generate minimal differences in size and B.E.T surfaces of resins. Additionally, the modification of polymerization's stirring velocity generates differences in polymer size, with a narrow distribution size between 200-400 rpm without a decrease in BET surface area. In comparison, the stirring material at velocities over 400 rpm, presents a broader size distribution of microparticles (but without an important decrease in B.E.T areas) until a total disappearance of spherical structure at 700 rpm as shown in the next SEM micrography, with a decrease around 300 m2g-1 . (Figure with morphological comparison was send in Author's response Reviewers)

With this previous result, it was decided to use a stirring speed of 400 rpm to obtain a narrow size distribution for the resin microparticles.

Major issues 3
In the manuscript, the characterization of the catalysts is sufficient. However, in the activity aspect, only insufficient results were provided. So, the authors should provide more results that can show their catalysts possess improved features including the activity compared to commercial or previously studied catalysts.

Answer: Sincerely grateful for the comment about the characterization techniques used in the present work. Concerning the catalytic activity, in the revised version of the manuscript, we have provided more detailed information and a comparison of catalytic results with previous reports. In particular, the PdAS(10)OS resin was tested in synthesizing Cinoxate and Octinoxate compounds as pharmaceuticals models to evaluate the Heck reaction performance.

Minor issues 1.
Minor errors include the wrong usage of comma, units, to non-scientific word placement.

Answer: Sincerely grateful for the comment. We reviewed this revised version carefully to improve the writing and compression of text.

Minor issues 2
The figure captions need to be redeemed, providing more details.

Answer: Sincerely grateful for the comment. We reviewed the figure caption to improve

	the information associated with the figures.

Manuscript number: app.20222758R1
TITLE: Immobilized Pd metal-complex on polymeric resin with high surface areas for recyclable catalyst: Effect of the immobilization method on nature of palladium species.

Dear Editor,

We are pleased to submit the revised version of the manuscript entitled “Immobilized Pd metal-complex on polymeric resin with high surface areas for recyclable catalyst: Effect of the immobilization method on nature of palladium species” to be considered for publication in the Journal of Applied Polymer Science. We sincerely thank to you and the reviewers for their valuable and constructive comments and corrections to our manuscript. The authors have carefully considered the comments and tried our best to address every one of them. The authors welcome further constructive comments if any. We have modified it accordingly, and the answers/comments are listed in detail herein, point by point. Finally, the corrections were marked in yellow in this revised version of the manuscript.

Sincerely,

Dr. Claudio Mella.
Postdoctoral researcher
Department of Polymer,
Faculty Sciences, University of Concepción
Edmundo Larenas 129, Concepción, Chile
Email: claudiomella@udec.cl

Reviewer #1: In the manuscript entitled "Immobilized Pd metal-complex on polymeric resin with high surface areas for recyclable catalyst: Effect of the immobilization method on nature of palladium species.", C. Mella et al. report a one-pot synthetic method and a multi-step for pseudo-homogeneous Palladium-based catalyst. In their methods, the palladium-coordinated monomers were converted to the catalytic polymer that can reuse and easily separated from the reaction mixture. Although the polymerization strategy using palladium coordinated monomers as a synthetic approach of supporting resin is novel, however, there are several major concerns regarding the catalytic efficiency of their palladium-encapsulated resins and the unclear scientific or technical advances. Thus, as long as the authors address the following issues, I do not have the enthusiasm to support its publication in Journal of Applied Polymer Science.

Major issues 1.

Considering their concept to fabricate a pseudo-homogeneous catalyst that has both reusability and improved catalytic activity compared to heterogeneous catalysts, the authors should demonstrate that the catalysts possess improved catalytic activity than the heterogeneous catalysts. Since palladium is located not only on the surface of the resin but also inside the resin, the catalyst activity is inevitably lost compared to homogeneous catalysts due to the diffusion problem of the reactants entering the resin. Thus, the main goal of fabricating a pseudo-homogeneous is to minimize the loss of activity and maximize reusability. Reusability was demonstrated in the manuscript. But they also need to show how much the activity was reduced compared to the same amount of homogenous catalysts and how their method minimized the decrease in catalytic activity.

Answer: Sincerely grateful for the comments. In the revised version of the manuscript, we provided information comparing the our catalyst with the usually reported homogeneous catalyst ($PdCH_3COO)_2$).

Major issues 2

The resin size might affect the activity of pseudo-homogeneous catalysts. So, if possible, the author needed to optimize the size of the resin.

Answer: Sincerely grateful for the comments; the study to optimize the size of resins was carried out previously in the context of Claudio Mella's doctoral thesis. The results demonstrate that different continuous phase/ discontinuous phase ratios generate minimal differences in size and B.E.T surfaces of resins. Additionally, the modification of polymerization's stirring velocity generates differences in polymer size, with a narrow distribution size between 200-400 rpm without a decrease in BET surface area. In comparison, the stirring material at velocities over 400 rpm, presents a broader size distribution of microparticles (but without an important decrease in B.E.T areas) until a total disappearance of spherical structure at 700 rpm as shown in the next SEM micrography, with a decrease around 300 m^2g^{-1} .

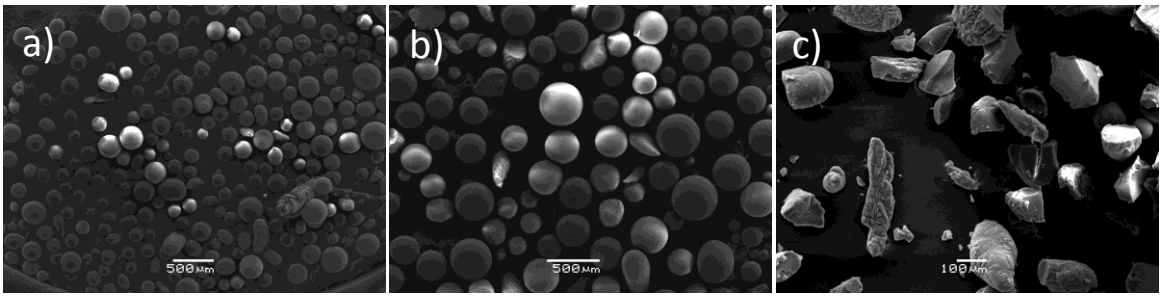

Figure. Morphological comparison by SEM analysis at different stirring velocities a) 400 rpm b) 550 rpm c) 700 rpm

With this previous result, it was decided to use a stirring speed of 400 rpm to obtain a narrow size distribution for the resin microparticles.

Major issues 3

In the manuscript, the characterization of the catalysts is sufficient. However, in the activity aspect, only insufficient results were provided. So, the authors should provide more results that can show their catalysts possess improved features including the activity compared to commercial or previously studied catalysts.

Answer: Sincerely grateful for the comment about the characterization techniques used in the present work. Concerning the catalytic activity, in the revised version of the manuscript, we have provided more detailed information and a comparison of catalytic results with previous reports. In particular, the PdAS(10)OS resin was tested in synthesizing Cinoxate and Octinoxate compounds as pharmaceuticals models to evaluate the Heck reaction performance.

Minor issues 1.

Minor errors include the wrong usage of comma, units, to non-scientific word placement.

Answer: Sincerely grateful for the comment. We reviewed this revised version carefully to improve the writing and compression of text.

Minor issues 2

The figure captions need to be redeemed, providing more details.

Answer: Sincerely grateful for the comment. We reviewed the figure caption to improve the information associated with the figures.

WILEY-VCH

Immobilized Pd metal-complex on polymeric resin with high surface areas for recyclable catalyst: Effect of the immobilization method on nature of palladium species.

Claudio Mella[1*], *Gina Pecchi*[1,2], *Cyril Godard*[3], *Carmen Claver*[3], *Abdiel Márquez*[4], *Cristian H Campos*[1]

[1]Facultad de Ciencias Químicas, Universidad de Concepción, Casilla Concepción 160-C, Chile,

[2]Millenium Nuclei on Catalytic Processes towards Sustainable Chemistry (CSC), Chile,

[3]Departmento de Química Física e Inorgánica, Universitat Rovira i Virgili, Tarragona, España.

[4]Centro de Nanociencias y Nanotecnología, Universidad Nacional Autónoma de México, Ensenada Baja California, México.

Correspondence to Claudio Mella, Postdoctoral research of Polymer Department, Universidad de Concepción, Casilla Concepción 160-C, Chile. E-mail: claudiomella@udec.cl

Keywords: Immobilization; synthetic route; palladium complex; metal-containing monomer.

Abstract

A critical query on literature is the approach used to immobilize homogeneous catalysts to improve their efficiency and recyclability. This work aims to compare the immobilization level of a kind of Pd-N,N'-bis(salicylidene)-o-phenylenediamine complex on high surfaces of polymeric resins to provide heterogenous catalysts for Mizorocki-Heck reaction. The preparation method involves two strategies: i) polymerization of the ligand before the complex-synthesis in a "multi-step (MS)" approach and ii) a direct "one-step" (OS) immobilization by polymerization of the metal-containing monomers (MCMs) as co-monomer. Both approaches effectively yield polymers with a larger surface area, over 700 m^2g^{-1}, and suitable thermic properties to use in the proposed reaction. In addition, the characterization of the polymers by XRD, XPS, and TEM demonstrates notable differences in Pd species on polymer support associated with the methodological approach to immobilizing the metal complex.

1. Introduction

The immobilization of metal coordination compounds has become essential for obtaining pseudo-homogeneous catalysts [1-3]. These catalysts take advantage of the excellent catalytic properties in terms of activity and selectivity of the homogeneous catalysts, with easy separation from the reaction medium and reusability [4-7]. Among different strategies for immobilization, covalent bonding is the most used methodology to obtain a stable, recoverable, and reusable immobilized coordination catalyst [8,9]. In this way, two different approaches have been established for the covalent immobilization of coordination compounds[10,11], as detailed in schematic 1. The first one (A) is called “multi-step synthesis” (MS), where the active phase is synthesized step by step until to obtain a surface-

immobilized coordination compound, while the second one (B) is called “one-pot synthesis” (OS) when the immobilization of the coordination complex is produced in situ.

Different inorganic and organic solids have been used to immobilize coordination compounds, such as SiO_2 [1,12-16], and Fe_3O_4 particles[17,18] , among others. Commonly, these inorganic matrixes needed surface grafting with linkers molecules to provide a covalent anchoring point for the immobilization of coordination compounds, which are generally focused on the MS approach. This approach presents a competitive effect between the adsorption of the metal precursor into the solid and metal coordinated by ligands on the surface. On the other hand, organic materials applied to metal coordination compound immobilization can be represented for metal-organic frameworks [18-20] and polymeric materials as covalent triazine frameworks[21], dendrimers, and polystyrene-based resins, as has been reviewed by Altava et al.[22]. Polymer matrixes are attractive materials to try the OS approach, especially using self-immobilization of metal-containing monomers (MCMs)[23-27], to keep control over the molecular structure of the metal coordination compound. Within the polymeric materials, the synthetic resin based on styrene (Sty) and divinylbenzene co-polymers [28-31], especially the commercial Merrifield resins[32-34], stand up for immobilization of coordination compounds due to its excellent thermal and mechanical properties. Additionally, Merrifield resins can be easily chemical modified; nonetheless, polymeric resin presents a drawback related to its limited surface area, which could result in a restrictive property to the accessibility[29] of the reactants to the active site, limiting their catalytic efficiency. Fortunately, the suspension polymerization methodology is a facile and economic methodology to obtain polymeric resins with a large surface area and controlled porosity [35-37].

Pd-based catalysts play a significant role in different organic reactions, acting as one of the essential organic synthesis tools. Therefore, many works have reported immobilized Pd-

coordination compounds [16,38-41]. Especially, Pd Schiff-bases metal complexes are employed as homogeneous catalysts in different reactions such as hydrogenation[42], epoxidation[43], carbonylation[44] and carbon cross-coupling[38,45-49], because there are highly stable and cheaper than typical Pd-phosphine complexes. Therefore, it is essential to develop the most suitable approach for immobilizing coordination compounds over polymeric matrixes to enhance their catalytic applications.

This work aims to synthesize and characterize immobilized pseudo-homogeneous catalysts into polymers with high surface area and their catalytic performance for the Mizorocki-Heck reaction. We propose that two methodological synthesis routes effectively obtain the Pd Schiff-base immobilized into surfaces of polymers with high surface area. We also report the textural, thermal, and spectroscopy evidence about coordination complexes immobilization and Pd-species. Finally, both materials were tested in the C-C coupling reaction to prepare cinnamic methyl ester starting from the methyl acrylate and iodobenzene at optimized reaction conditions. The best-immobilized catalyst was compared with the usually homogeneous catalyst, $Pd(CH_3COO)_2$, used for the Heck reaction. Additionally, to ensure the scope of the reported catalyst, the production of Octinoxate and Cinoxate were carried out from their corresponding building blocks.

2. Materials and Methods

2.1. *Materials*

Sodium chloride, palladium (II) acetate $Pd(CH_3COO)_2$, ethanol absolute (EtOH), n-hexane, iodobenzene (IB), iodoanisole ($IBOCH_3$), 2-ethylhexyl acrylate (EHA), 2-ethoxyethyl acrylate (EEA) and acetone (99.5%) were purchased from Merck®. Hydroxyethyl-cellulose (HEC, 99%, ~90000 MW), 3-allylsalicylaldehyde (97%), o-phenylenediamine (99.5%), and

divinylbenzene (DVB, technical grade 80%) were purchased from Sigma Aldrich®. Methyl acrylate (MA, 99% Aldrich®) was distilled at normal pressure in the presence of p-tert-butylcatechol as an inhibitor; 2,2'-azobisisobutyronitrile (AIBN, Aldrich®) was purified by recrystallization from methanol; dichloromethane (DCM, 99% Merck®) was dried with CaH_2; toluene (≥ 99.0% Merck®) was dried over Na(s) and distilled previously to use.

2.2 Characterization techniques

Chemical analysis of the samples was conducted by inductively coupled plasma optical emission spectrometry (ICP-OES) using a Spectro Arcos instrument. The preparation of the samples included an HNO_3 and H_2SO_4 microwave acid treatment on a Milestone Srl model Ethos Easy and then diluted for further analysis.

Thermogravimetric analysis (TGA) was performed at a heating rate of 10°min-1 up to 900°C with N_2 flow of 8.0 mL/min in NETZSCH TG instrument model 209F1 Iris, using 3.0 mg of sample.

The ^{13}C decoupling, ^{1}H NMR, C-H correlation NMR, and solid-state ^{13}C CP-MAS NMRs analysis were performed on a Mercury VX400 VARIAN.

Nitrogen adsorption isotherms at a temperature of -196°C were obtained on a Micromeritics apparatus Model TriStar II Series 2; the specific area was calculated using the B.E.T method, while the pore size distribution and pore volume by BJH method.

SEM and TEM characterized the morphology of the samples; the first one was on an SEM-Probe CAMECA model SU-30 coupled to an EDS probe, and the second was on a Jeol JEM-1200 EXII. Gaussian distribution analysis of the diameter of 600 particles was used to estimate the average particle diameter.

A Bruker FT-IR model Vertex 70 was used for FT-IR analysis. A Thermo Scientific Bio UV-Vis Spectrophotometer model Evolution 260 was used for UV-VIS spectroscopy analysis.

Elemental analysis of AS ligand and Pd-AS metallo-monomer were characterized on a Sartorius balance model M2P and Perkin Elmer Elemental analyzer model EA2400.

XPS measurements were performed using a VG Escalab 200R electron spectrometer equipped with a hemispherical electron analyzer and Mg Kα (1253.6 eV) as the X-ray source.

Lastly, XRD patterns were obtained with nickel-filtered CuKa1 radiation (λ=1.5418 Å) on a Rigaku diffractometer and collected from the range of 20-90° for 2Θ.

2.3 Synthesis of AS and PdAS.

Schematic 2 shows the AS ligand and PdAS MCM synthesis route. A typical synthesis involves the dissolution of 40.0 mmol of 3-allylsalicylaldehyde on EtOH mixed with a dissolution of 20.0 mmol o-phenylenediamine in 50 mL of EtOH refluxed for two hours. Then, the mixture was cooled, and the resultant solid was recrystallized from EtOH to obtain the orange solid ligand AS[50]. For PdAS MCM synthesis, the AS ligand was dissolved in a solution of dichloromethane and $Pd(CH_3COO)_2$, using a 1:1 ratio between Pd and AS. The mixture was stirred for 12 hours to obtain a brown solid, washed after, and recrystallized on the DCM/n-hexane mixture.

2.4 Synthesis of PdAS(10) MS and PdAS(10) OS resins.

The literature suggests that the resin synthesis must be in a three-neck polymerization reactor [29,51]. The synthesis involved 60, 29, 10, and 1 wt.% of DVB, MA, AS (or PdAS), and AIBN:

1. The co-monomers and initiator were mixed and stirred for 10 min.
2. Toluene was added to the mixture and kept for 10 min under stirring.
3. The mixture was suspended over an aqueous phase in a three-neck polymerization reactor (containing 20 wt.% of NaCl and 0.2 wt.% of HEC) at 400 rpm mechanical stirring.

The polymerization was carried out at 70°C for 14 hours and 88°C for 4 hours under N_2 flow (10 mL·min^{-1}).

.For MS methodology, the yellow polymer beads were washed with water and acetone for 48 hours in a Soxhlet extractor and dried at 83°C in a vacuum oven. Materials were denominated AS(10) resin. AS(10) resin was contacted with an excess of $Pd(CH_3COO)_2$ solution in DCM (with 1:1.1 nominal molar ratio AS on polymeric materials in $Pd(CH_3COO)_2$ for 12h, washed with DCM, and dried on a vacuum oven overnight, to obtain brown PdAS(10)MS resin.

With the OS approach, brown beads of PdAS(10)OS resin were obtained by self-polymerization of PdAS and washed in a Soxhlet extractor with water and DCM. Then, the acquired resin PdAS(10)OS beads were dried at 83°C in a vacuum oven.}

2.5 Catalytic evaluation.

The catalytic Heck coupling reaction of IB and MA to obtain methyl cinnamate (MCIN) was evaluated as a test reaction, and the most promising catalyst was evaluated in the recycle test. In a typical reaction, 50 mg of catalyst was dissolved on specific precursors based on the desired amount of Pd. The reactant conditions were IB:Pd 2000:1 and IB:MA:TEA 1:1.25:2.

The reaction was carried out in a Parr-type semi-batch reactor at 120°C in Ar (5.5 bar), at 770 rpm of magnetic stirring, using 50mL of DMF as solvent, and dodecane as the internal standard. The catalytic activity was measured at different times. Identical catalytic conditions were performed using the corresponding $Pd(CH_3COO)_2$, iodoarenes and acrylates reactants to evaluate the Heck reactions.

The samples were taken over 1 mL of water, followed by extraction with Et_2O (1000 µL) and washing with 1 mL of brine. The conversion was measured in terms of IB consumption, analyzing the organic layer at a Perkin Elmer GC model Clarus 680, equipped with an Elite-MS5 capillary column. Additionally, the leaching evaluation was carried out by analysis of the post-reaction catalytic mixture. The Turn Over Frequency (TOF) evaluation of catalysts was calculated using the initial velocity and considering all the palladium amount disposable into the materials as a catalytic atomic single site.

3. Results and Discussion.

3.1. AS and PdAS characterization.

Pure AS ligand was obtained as an orange solid with 80% yield after recrystallization. The ^{1}H -^{13}C HSQC NMR spectra (400 MHz, $CDCl_3$, 25 °C) of the AS shown in Figure 1a confirms the AS structure with the characteristic peaks at 3.45, 5.06, 5.09, and 6.06 ppm related to allyl groups. The peaks between 6.86 to 7.34 ppm are associated with an aromatic structure. The protons peaks of imine and alcohol appear at 8.63 and 13.3 ppm, respectively, according to He *et al*[50]. The orange line in the FT-IR spectra in Figure 2a shows the expected band associated with hydroxile and imine distinct groups, corresponding to AS ligand at 3440 (-OH) and 1614 cm^{-1} (-C=N-) [50,52]. In addition, the orange line of UV-Vis spectra

(DCM) shown signals at 229 and 278 nm related to typical π → π* transition of aromatics ring and azomethine group and n → π * transition at 341 nm.

In Figure 1b, the $^{1}H–^{13}C$ HSQC NMR spectra (400 MHz, $CDCl_3$, 25 °C) of PdAS demonstrate the obtention of PdAS MCM without decomposition of ligand, with the expected disappearance of the -OH signal. In the FT-IR spectra of the PdAS coordination compound, the black line in Figure 2a, the characteristic displacement of the wave number of imine band to 1602 cm^{-1} (-C=N-), and the disappearance of the signals related to OH confirmed the PdAS formation.

UV-Vis spectra (DCM) in Figure 2b show the signals of aromatic π → π* transition band at 244 nm, π → π* and n → π * transition bands between 336 and 355 nm, with a bathochromic shift by metal center coordination, confirmed by the apparition of a new transition at 481 nm related with charge-transfer (C-T)/ d-d transition[53,54].

Figure 3 shows the wide XPS spectrum range, identifying the binding energies and auger emissions for the surface atomic components on the PdAS coordination complex. Only one surface Pd $3d_{5/2}$, at 339.60 eV, and a spin-orbital splitting of 5.27 eV for the $3d_{3/2}$ component was detected. This Pd surface specie was compared with the $Pd(CH_3COO)_2$ precursor that present BE at 338.4 eV for $3d_{5/2}$ and 343.7 for $3d_{3/2}$ core level.

The spectroscopy data confirms the formation of AS ligand and PdAS coordination compound with two polymerizable groups. In addition, the organic elemental analysis of AS and PdAS summarized in Table 1 confirms the expected chemical formula.

3.2 AS(10), PdAS(10) MS and PdAS(10) OS resins characterization

Figure 4 demonstrates the N_2 adsorption-desorption isotherms of the PdAS(10)OS, PdAS(10)MS immobilized Pd polymers, and the AS(10)resin. All materials exhibited isotherm with narrow hysteresis loop at high pressure, classified as type IV on IUPAC classification, characteristic of mesoporous materials or interstitial spaces in agglomerates of nanoparticles. Table 2 displays the surface areas over 700 m^2g^{-1}. AS(10) resin did not show significant changes in textural properties after contact with $Pd(CH_3COO)_2$ on both resin precursor and PdAS(10)MS; with pore diameter near 13 nm and a minimal increase in the surface area related to a more surface exposed in broken material.

On the other hand, PdAS (10)OS resin showed a significant increase in surface area and mean pore diameter. The differences in pore diameter can be related to a different monomer mixture's solubility on single drop-in presences or absences of metallic center coordinated directly on an AS monomer[36].

TGA measure for the immobilized polymers presents high decomposition temperature, as shown in the thermal decomposition profile in Figure 5. This elevated decomposition temperature is associated with the high crosslinked grade of synthesized polymers with T_{50} at 451 and 442°C for PdAS(10)OS and PdAS(10)MS resins, respectively[55].

SEM micrographs for AS(10) resin in Figure 6a picture the expected spherical morphology for a typical suspension polymerization process. By Gaussian distribution (inset of Figure 6a) was possible estimated an average diameter value of 216 μm.

This regular morphology for crosslinker resin was broken entirely after contact with $Pd(CH_3COO)_2$ to form PdAS(10)MS resin, as shown in Figure 6b. A similar result has been reported for Jadhav for an immobilized Pd catalyst prepared by M.S approach, passing from well-defined microparticles to powder kind material[33,56]. Additionally, the

surface EDS techniques in Figure 7 showed obtaining 0.5% Pd to broken PdAS(10)MS resin and 1.2% Pd to spherical PdAS(10)OS resin, respectively. ICP-OES measured similar trends in Pd loading, with 0.7 wt.% for PdAS(10)MS and 1.4 wt.% for PdAS(10)OS. These values indicate that the OS approach immobilizes twice the Pd amount compared to the MS methodology.

Figure 8a displays the solid ^{13}C CP-MAS NMR spectra for PdAS(10)MS and PdAS(10)OS. The principal signals are related to the DVB[57] main component that masks the principal signals of the coordination compound in the aromatic zone and the central polymer backbone at 33 ppm, as well as the methyl moieties of ethylbenzene technical grade DVB. In addition, it is possible to distinguish two signals attributed to the MA component in the polymer, the first one as a shoulder at 58 ppm related with $–OCH_3$ moiety and the second one of the carbonyl group at 184 ppm.

FTIR spectra in Figure 8b show the same evidence; the influential absorption bands of C=O mask the Pd Schiff Base immobilized signal at 1739 cm^{-1} and C-O tension at 1164 cm^{-1} characteristic of MA, and the signals of aromatic vibrations of the polymer. The only band associated with the Schiff-Base complex appears at 796 cm^{-1}, with no clear evidence to confirm the nature of Pd in the immobilized polymers. These are notable differences from others immobilized palladium complexes reported in the literature that FTIR analysis can identify.

The XPS analysis shed light on the chemical environment of surface palladium species in the PdAS(10) resins and has a comparison point concerning the PdAS-free complex. Figure 9a shows the Pd 3d spectra of the PdAS(10)MS and Figure 9b for PdAS(10)OS polymers. The spectra of Pd 3d for PdAS(10)OS fits a Pd $3d_{5/2}$ at 339.40 eV and Spin-orbital

splitting at 5.3 eV, denoting one Pd oxidative state. Conversely, in the PdAS(10)MS, the deconvolution indicates at least two Pd oxidative states, the first at 336.1 eV typically attributed to the Pd^0 component and the second at 338.1 eV related to the Pd^{2+} component associated with $Pd(CH_3COO)_2$ precursor BE[58]. This mixture of Pd species can be understood due to the long-time of reaction and an impossibility to proceed to the metal complexation reaction, producing a reduction of $Pd(CH_3COO)_2$ precursor, similar to the effect for the same metallic precursor and comparative polymer matrix was reported previously by Mathew [59]. Therefore, the OS approach allowed the synthesis of the PdAS complex immobilized on polymers with high surface areas.

TEM characterization results reinforced the differences between MS and OS approaches. It is possible to see nanoparticles on the polymer surface for PdAS(10)MS in Figure 10a. Additionally, the electron diffraction pattern (inset of Figure 10a) was measured, obtaining the *d*-spacing values of 0.224; 0.193; 0.137, and 0.112 nm, coinciding to (111), (200), (220), (311) and (222) planes of palladium nanoparticles. Unlike PdAS(10)MS, PdAS(10)OS did not show metal particles on the surface or a diffraction pattern in electron diffraction analysis. The XRD analysis in Figure 11 exhibits the typical broad signals associated with the non-crystalline structure of crosslinked polymer matrix at 19° 2θ value[60] and a second shoulder around 43° 2θ value. Furthermore, for PdAS(10)MS is possible to see the planes of diffraction associated with metallic Pd according to TEM characterization and XPS spectra.

3.3 Catalytic evaluation.

Both catalysts showed high catalytic performance of iodobenzene and methyl acrylate coupling reaction in Figure 12a. The PdAS(10)MS completed the reaction in 5 min, while the PdAS(10)OS catalyst showed a progressive conversion that reached 99% of conversion at 30

min. After the every reaction, the leaching test was performed to evaluate the operational stability of both catalysts. The analysis revealed that the PdAS(10)MS leached 14,7% of the total Pd onto the resin's surface, while the PdAS(10)OS did not display Pd on the supernatant after the first catalytic cycle. These results demonstrate that the post-synthesis of the Pd species onto the resin surfaces provides unstable heterogeneous catalysts compared to the use of a metallo-monomer in the resin preparation. In addition, PdAS(10)OS was compared to the homogeneous $Pd(CH_3COO)_2$, which is the commonly used catalyst for Heck reaction[61]. The heterogeneous PdAS(10)OS shows a TOF = 6122 h^{-1} instead of $Pd(CH_3COO)_2$ that displayed a TOF = 29554 h^{-1} at the same reaction conditions. As expected, the homogeneous catalysts have improved performance compared to the heterogeneous PdAS(10)OS system. However, this catalyst is efficient and stable at least in 4 catalytic cycles, as displayed in Figure 12b. After the fourth continuous catalytic cycle, the catalysts displayed negligible Pd leaching (~7.6%).

Additionally, Table 3 presents the results for the catalytic performances of various Pd-supported onto polymeric matrix as catalysts for the Heck reaction. The TOF values were considered to compare the catalytic performance. Among them, Ma *et al*[62] and Nagai *et al*[63] reported high catalytic performance for the Heck reaction using IB and MA to produce MCIN reaching a TOF of 16,000 and 13,889 h-1, respectively, which is 2.5-fold higher than our proposed catalytic system. These high catalytic activities are attributed to the nature of the polymer component in the catalyst system, which corresponds to the soluble macromolecules stabilizing the Pd^{II}-based active site. However, in the case of heterogeneous catalysts reported by Mahmoudi *et al*[64] and Balinge *et al*[65], the catalytic activity displayed an important decrease providing TOF values between 0.02 to 0.03-fold lower than our reported catalyst.

Owing to the excellent recyclability and good catalytic activity of the PdAS(10)OS system, it was further evaluated for the Heck reaction of other iodoarenes and alkenes, which

are relevant building blocks for the synthesis of pharmaceutical compounds. The operational conditions for the heck reaction were identical to those used for the test C-C coupling. Table 4 shows the conversion and selectivity for the corresponding products, indicating that all of the C-C heterocoupling reactions were successfully produced only the desired isomer. In the case of entries 3 and 4, both products are used by the pharmaceutic industry because they are used as approved active agents in UV-A and UV-B sunscreen approved by U.S. Food and Drug Administration (FDA). The PdAS(10)OS was applied to synthesize Octinoxate by catalytic coupling of $IBOCH_3$ and EHA, obtaining 7.28g of Octinoxate after 3 consecutive catalytic cycles; this result is comparable with the efficiency reported by Hamasaka *et al.* using homogenous palladium NNC-pincer complex[39]. In addition, the cinoxate preparation by coupling $IBOCH_3$ and EEA was also successfully reaching 6.87 g after 3 consecutive catalytic cycles. Thus, our results provide a valuable and practical method by which cinnamate-based pharmaceutical relevance commodities can be obtained via Heck reaction using Pd^{II}-based heterogeneous catalyst.

4. Conclusion.

This work provides solid evidence about the differences in the synthesis approach used to immobilize the PdAS complex in a polymeric resin with a high surface area. Different characterization techniques discarded our thesis of obtaining the same catalytic specie by different synthesis routes. The leaching test and possible reuse of PdAS(10)OS resin in consecutive catalytic cycles demonstrates the differences in the supported species in the polymer surface and their impact on catalytic performance.

Moreover, we can ratify that self-polymerization is the most efficient approach to immobilizing PdAS MCM, avoiding the metal nanoparticle aggregation and the leaching process in catalytic tests. Ultimately, the polymeric resin obtained by self-polymerization

exhibits superior performance in consecutive cycles of the Heck coupling reaction, capable of standing up to four cycles.

5. Acknowledgement.

In memory of Professor José Luis Garcia Fierrro. The authors would like to thank J.L.G. Fierro for his contribution to this work, and specifically his significant contribution to the XPS field. The authors thank to CESMI, Universidad de Concepción, for microscopy and NMR analysis. C.Mella acknowledges support from ANID FONDECYT 3200379; G. Pecchi acknowledges support from ANID FONDECYT 1210142.

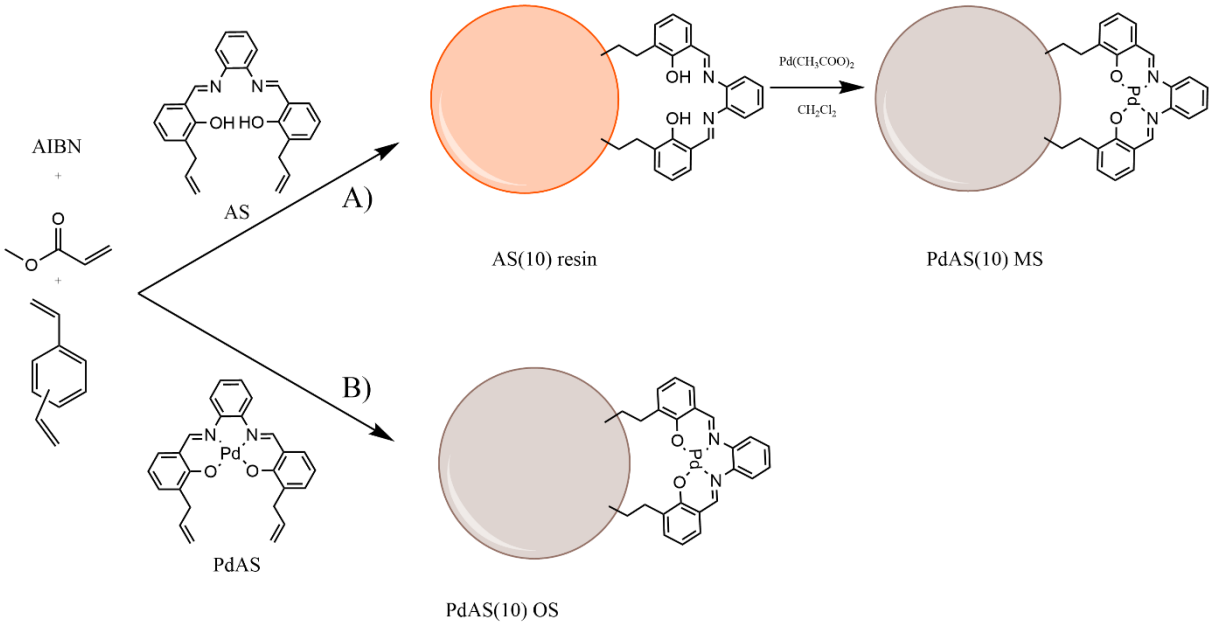

Scheme 1. Synthesis pathways evaluated to the immobilization PdAS complex onto polymeric resins.

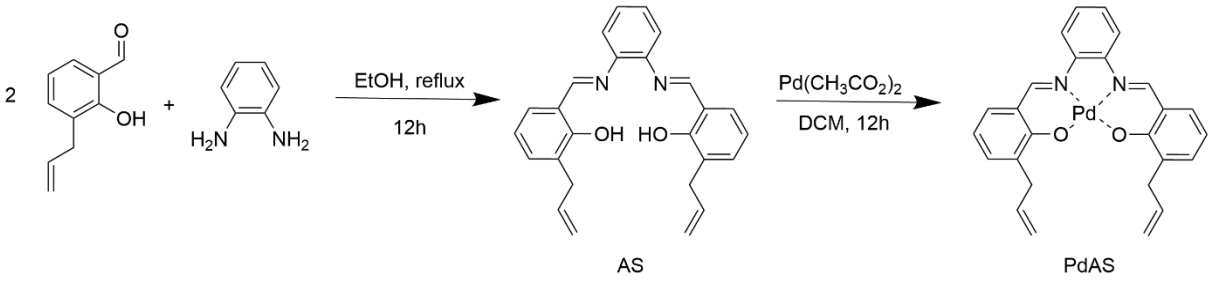

Scheme 2. Scheme of the synthesis of AS monomer and PdAS metallo-monomer.

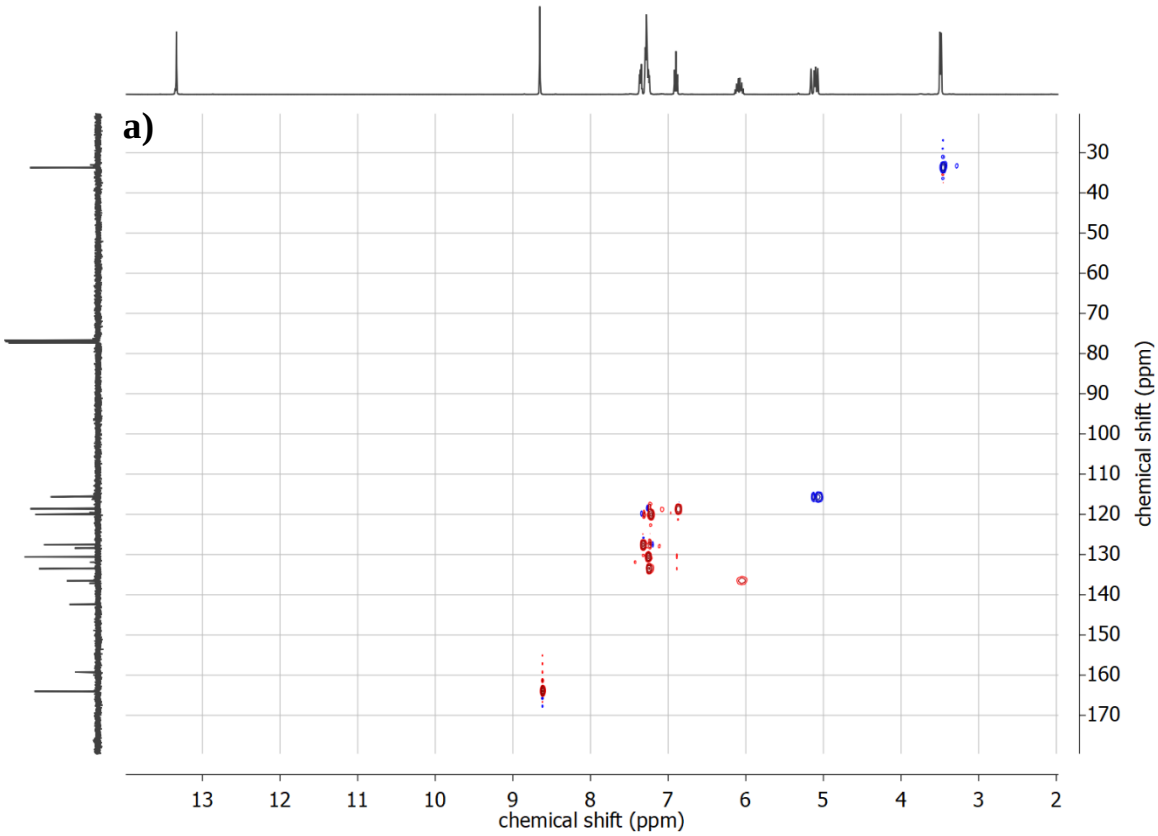

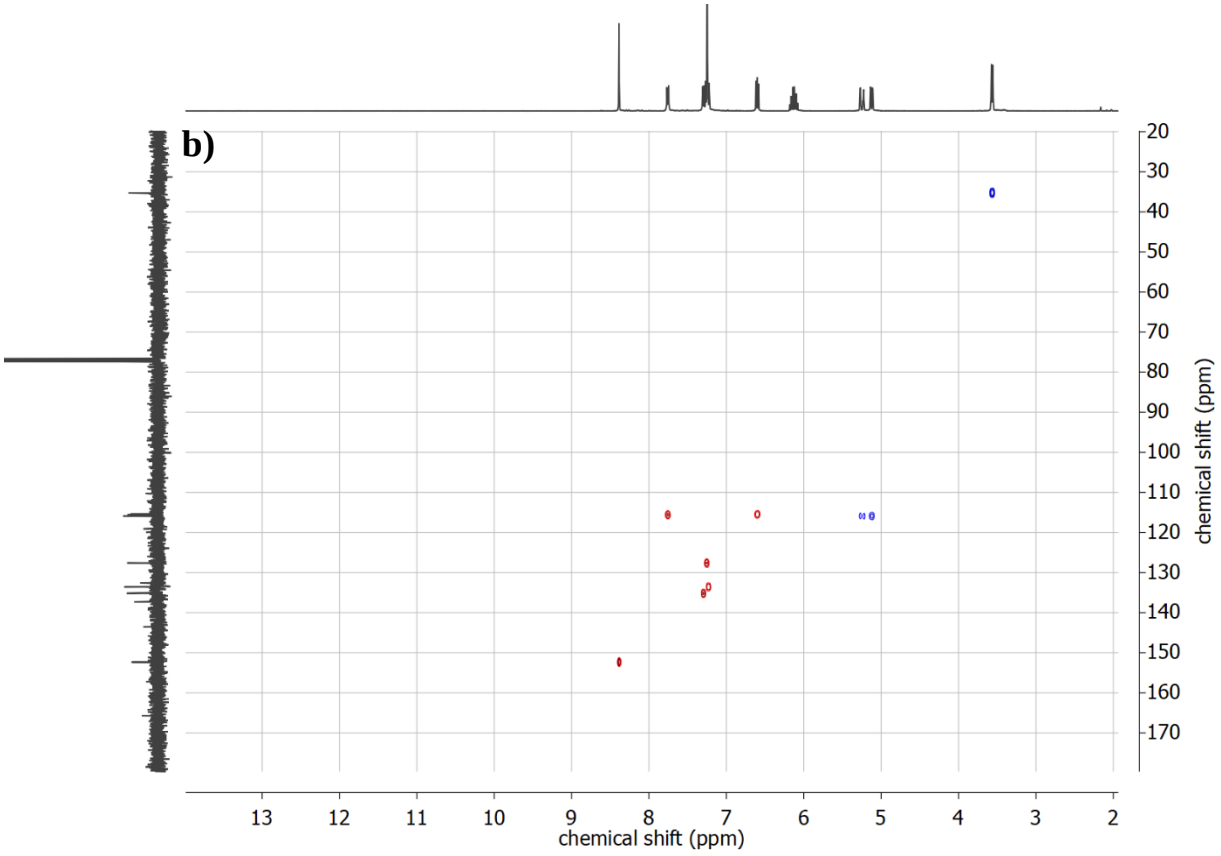

Figure 1. ^{1}H-^{13}C HSQC NMR experiments in $CDCl_3$ for the preparation of (a) AS monomer and (b) PdAS metallonomnof.

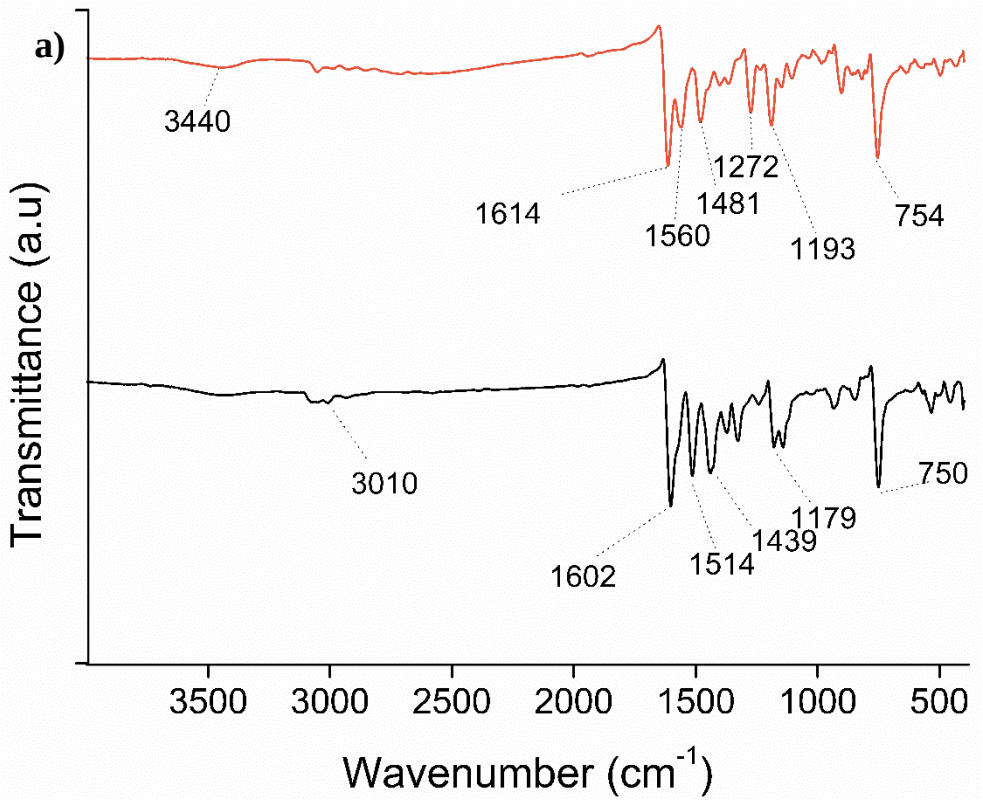

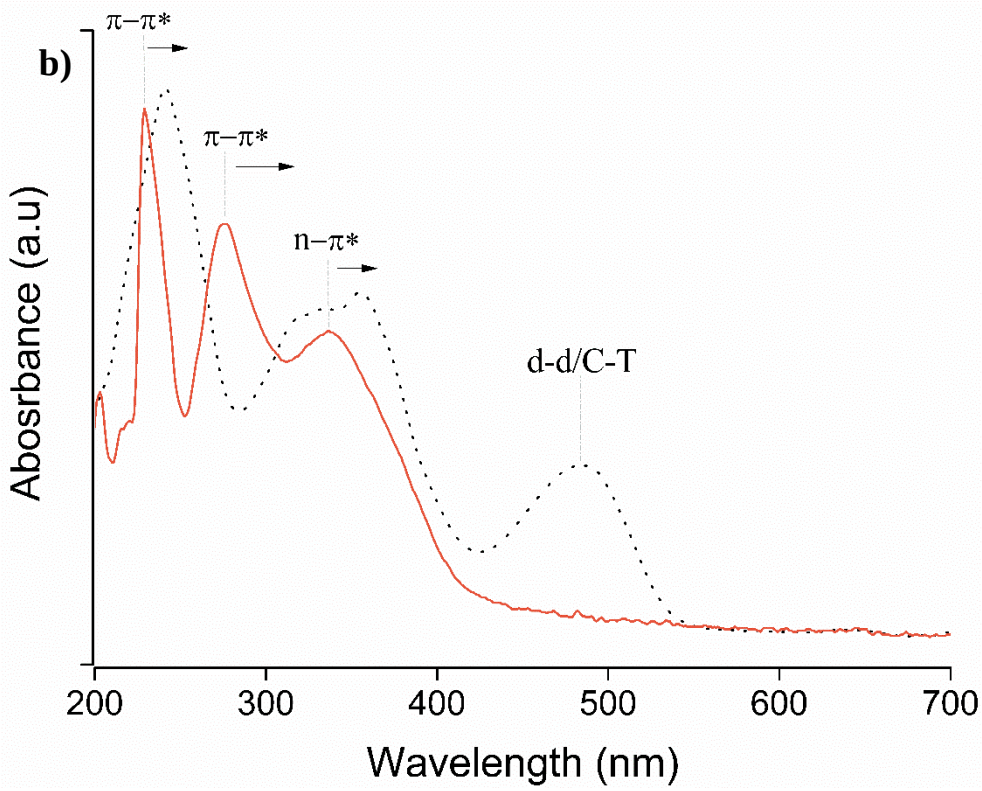

Figure 2. Spectroscopy characterization of AS free ligand and PdAS MCM by. a) FTIR Spectra in KBr pellet. b) UV-Vis spectra on CH_2Cl_2 as solvente

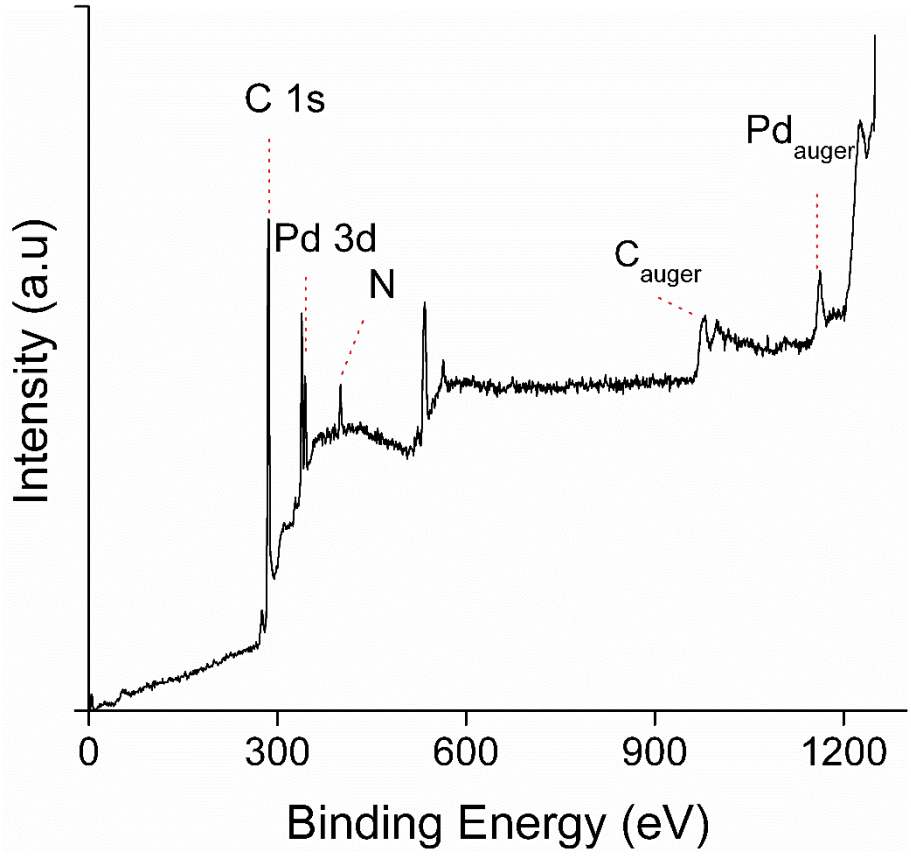

Figure 3. XPS survey spectra of PdAS metallo-monomer.

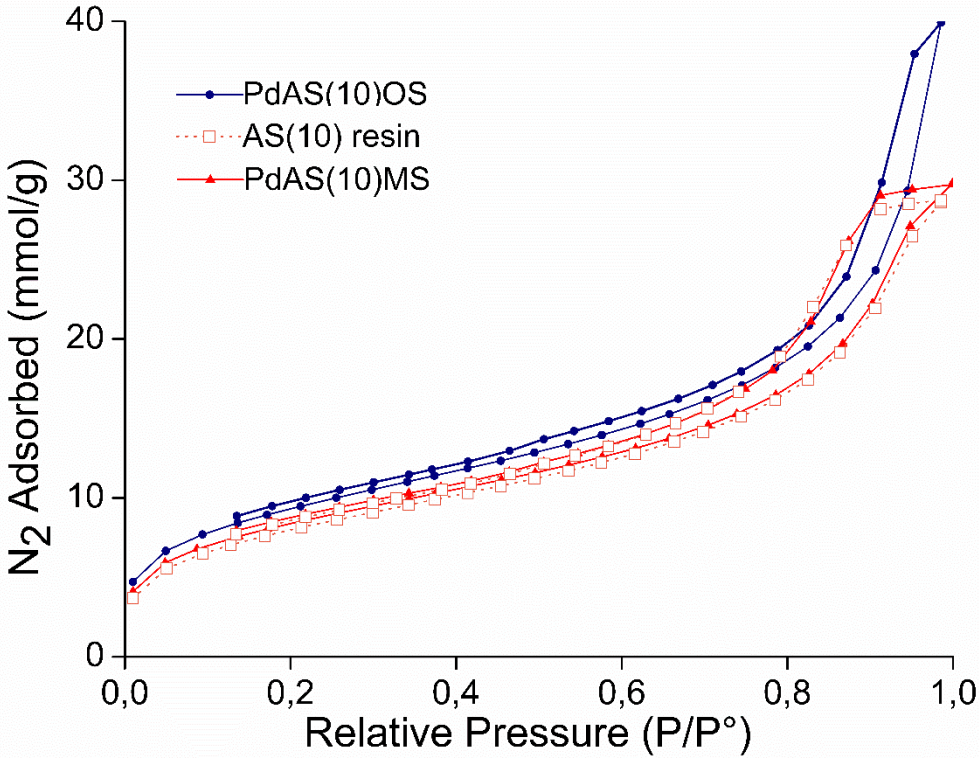

Figure 4. N_2 adsorption-desorption isotherms at -196°C for the synthesized materials.

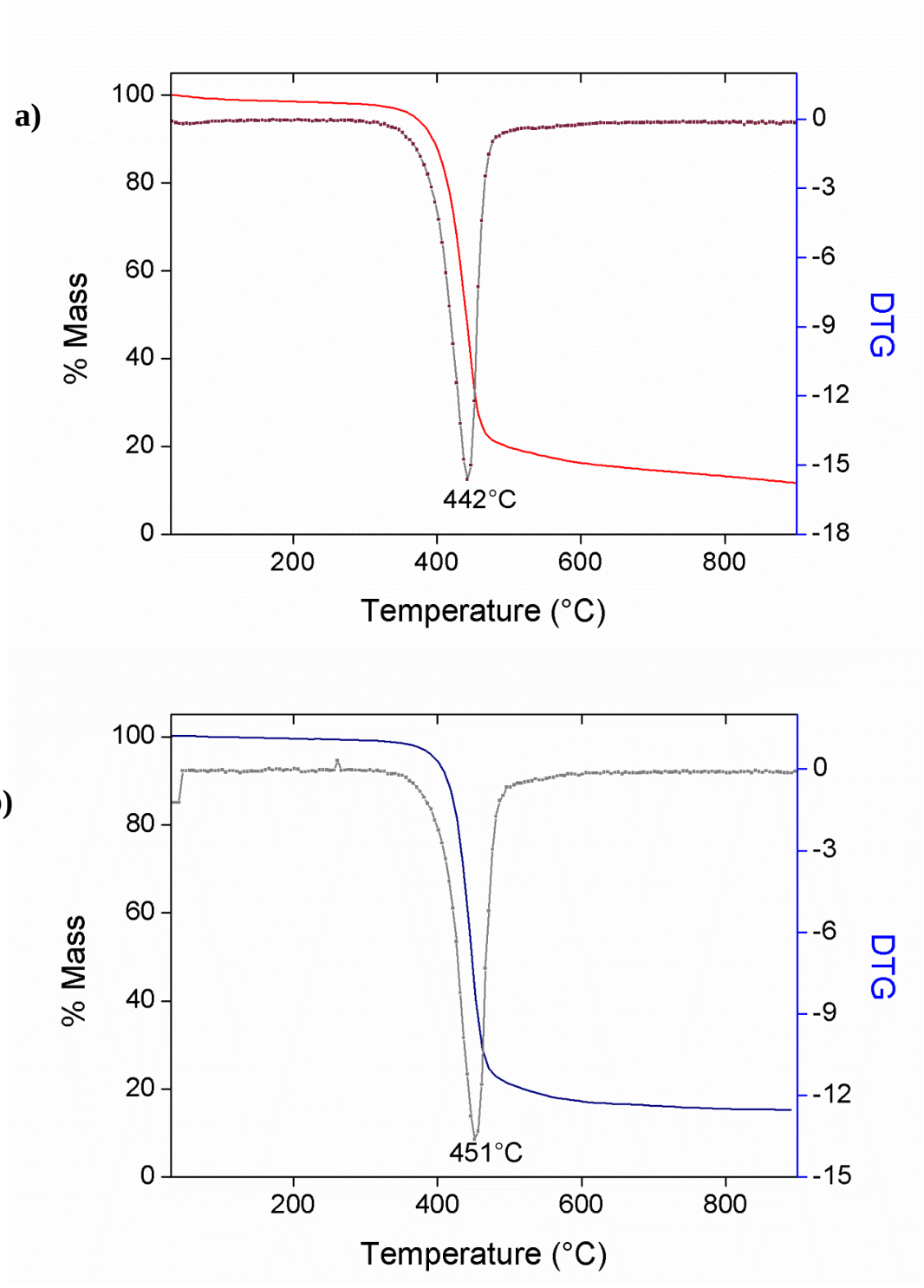

Figure 5. Thermogravimetric profile, using a heat ramping of 10°C/min from RT to 900°C, in N_2 atmosphere for (a) PdAS(10)MS (b) PdAS(10)OS.

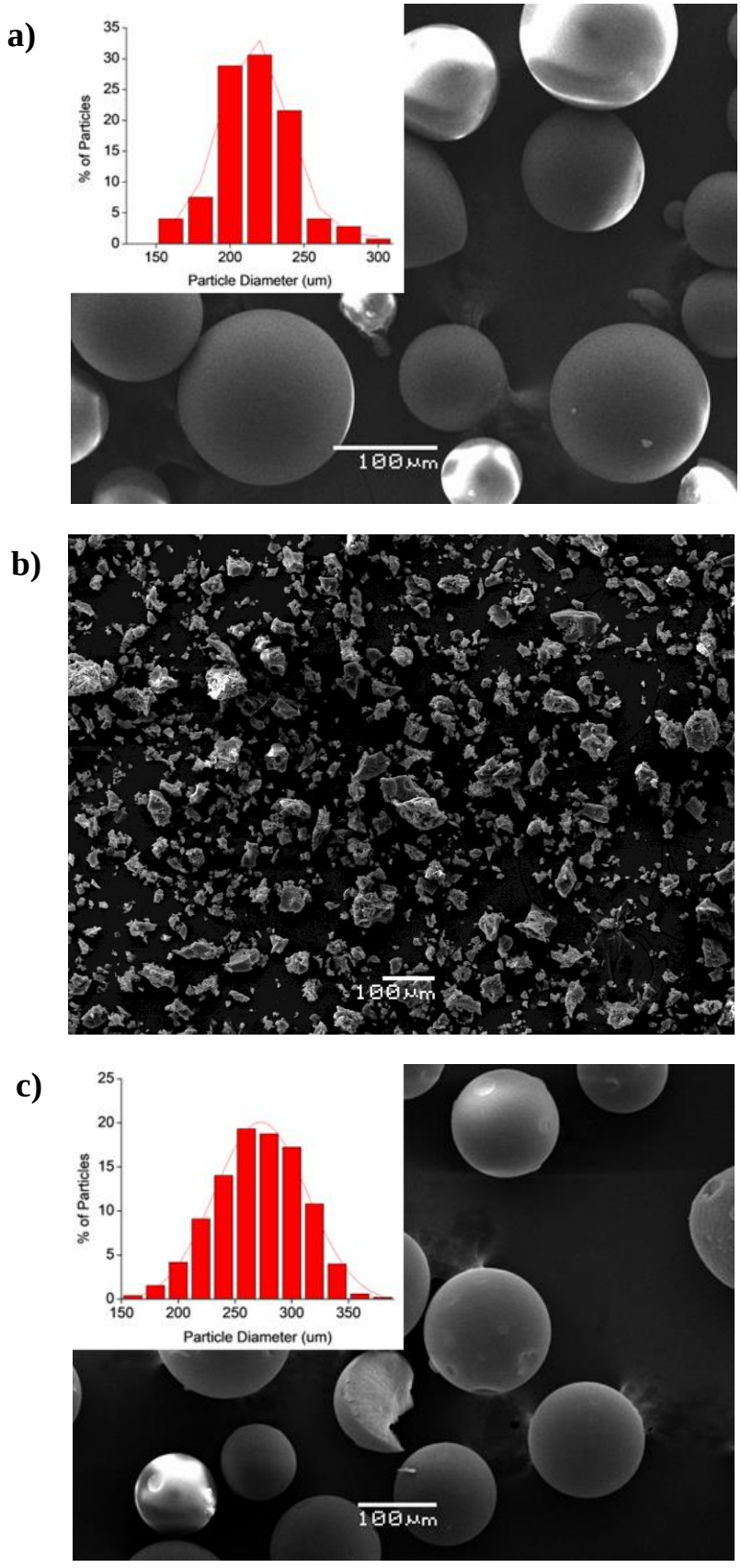

Figure 6. SEM micrographs and main spherical size distribution for synthesized materials (a)AS(10) resin (b)PdAS(10)MS (c)PdAS(10)OS.

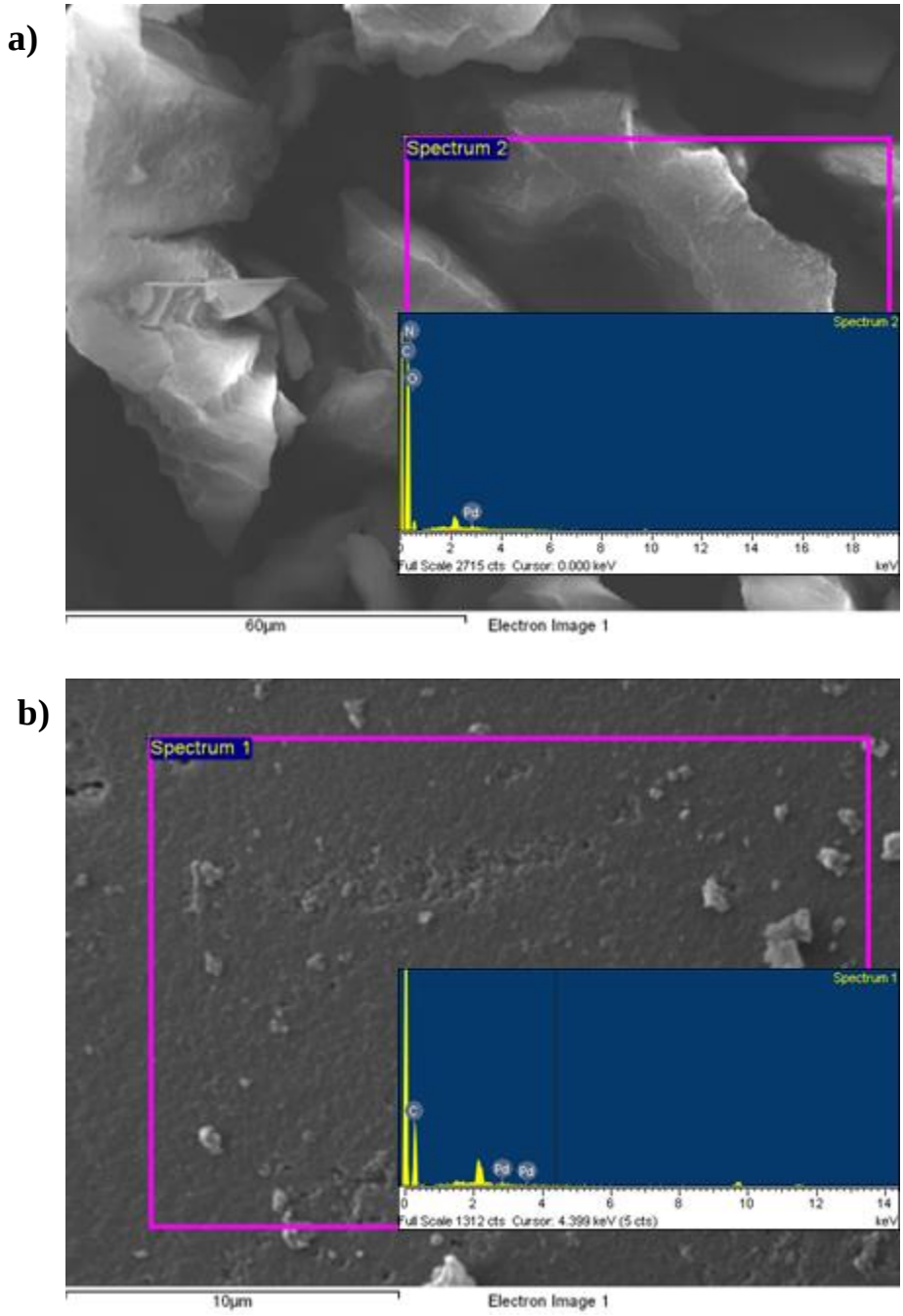

Figure 7. EDS analysis from SEM micrographs for synthesized materials (a)PdAS(10)MS and (b)PdAS(10)OS.

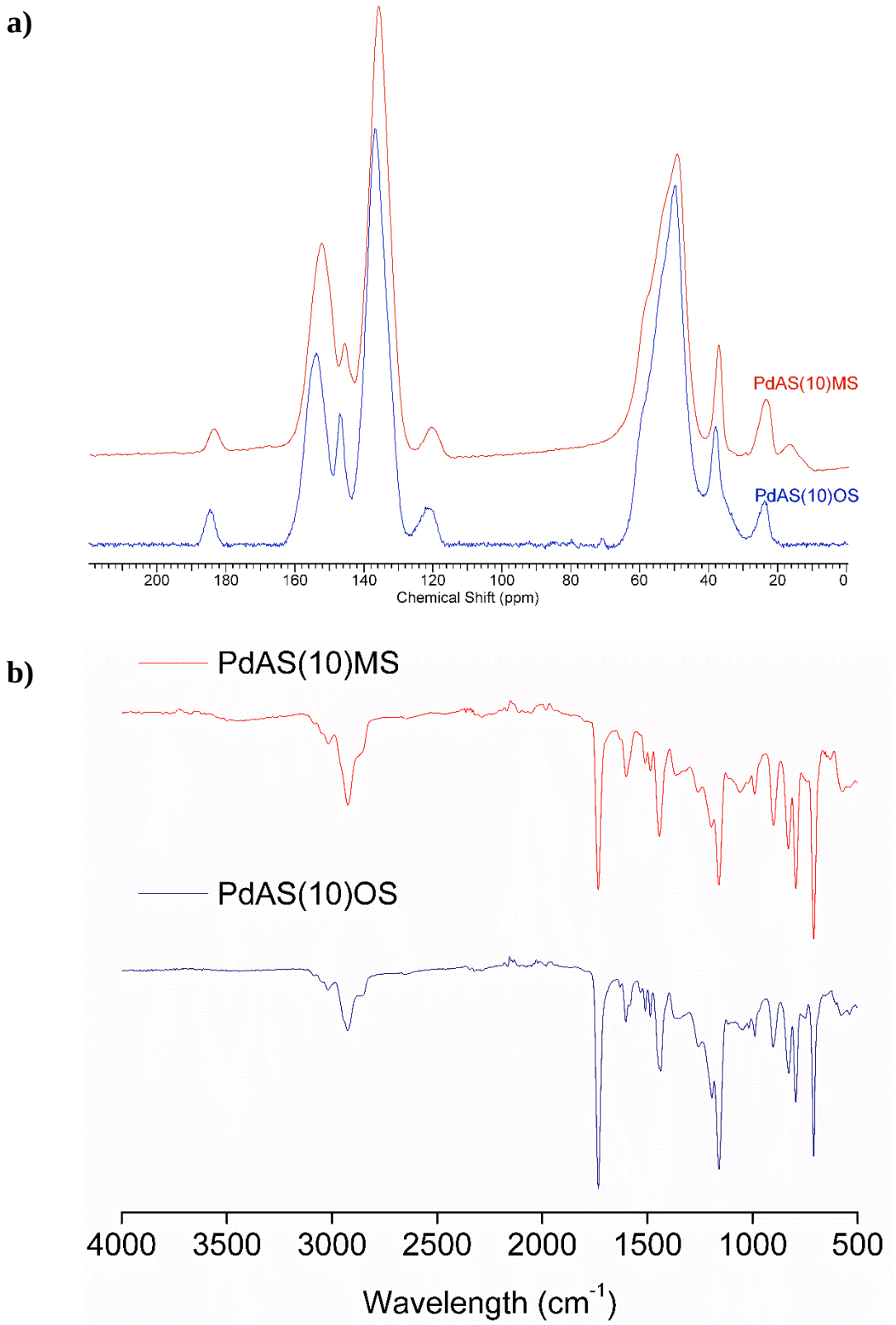

Figure 8. Spectroscopy characterization of PdAS(10)MS and PdAS(10)OS by (a)^{13}C-CP MAS NMR in solid state (b) FTIR.

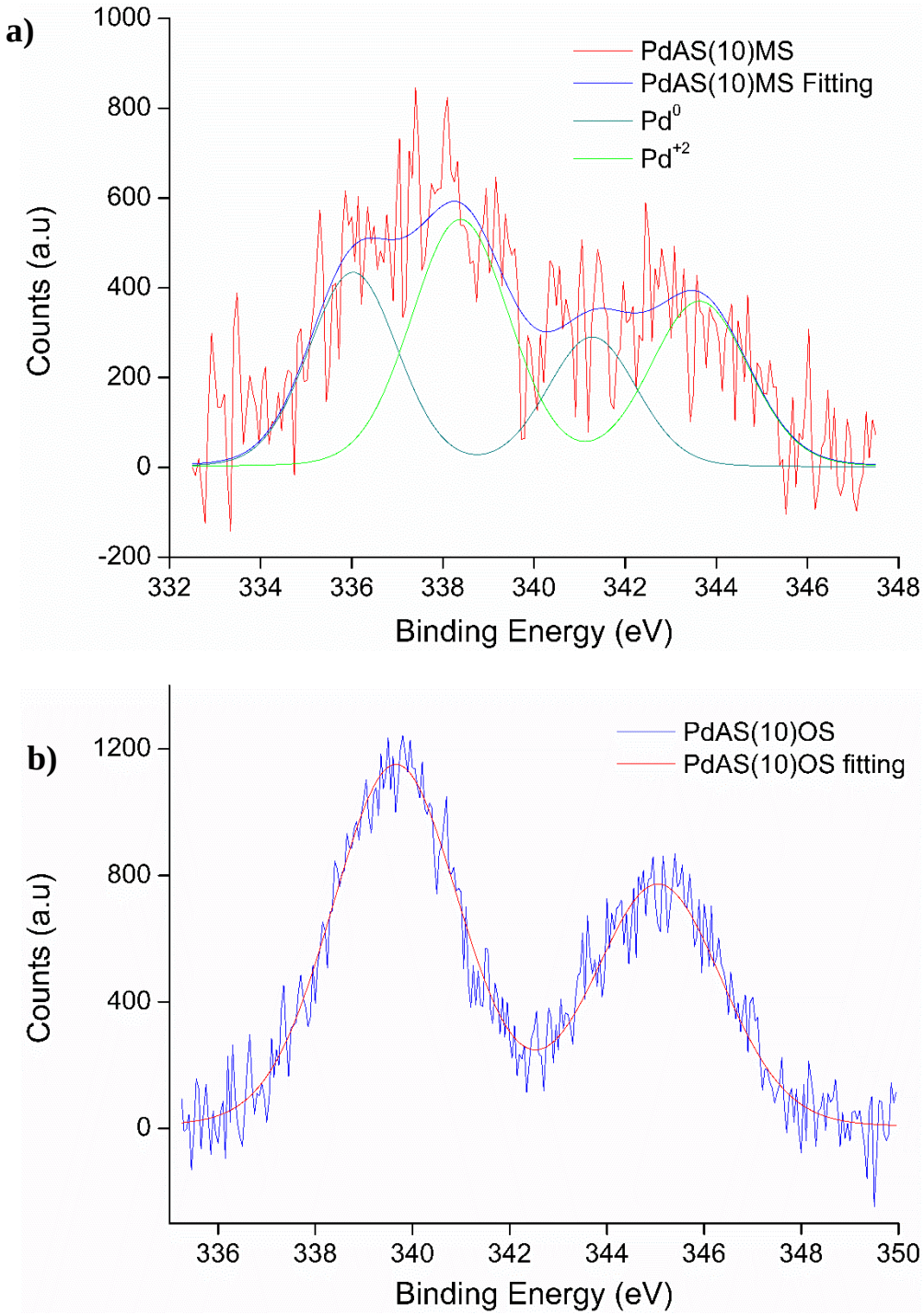

Figure 9. High-resolution XPS spectra of Pd 3d and curve fitted peaks for the synthesized materials. a)PdAS(10)MS. b)PdAS(10)OS.

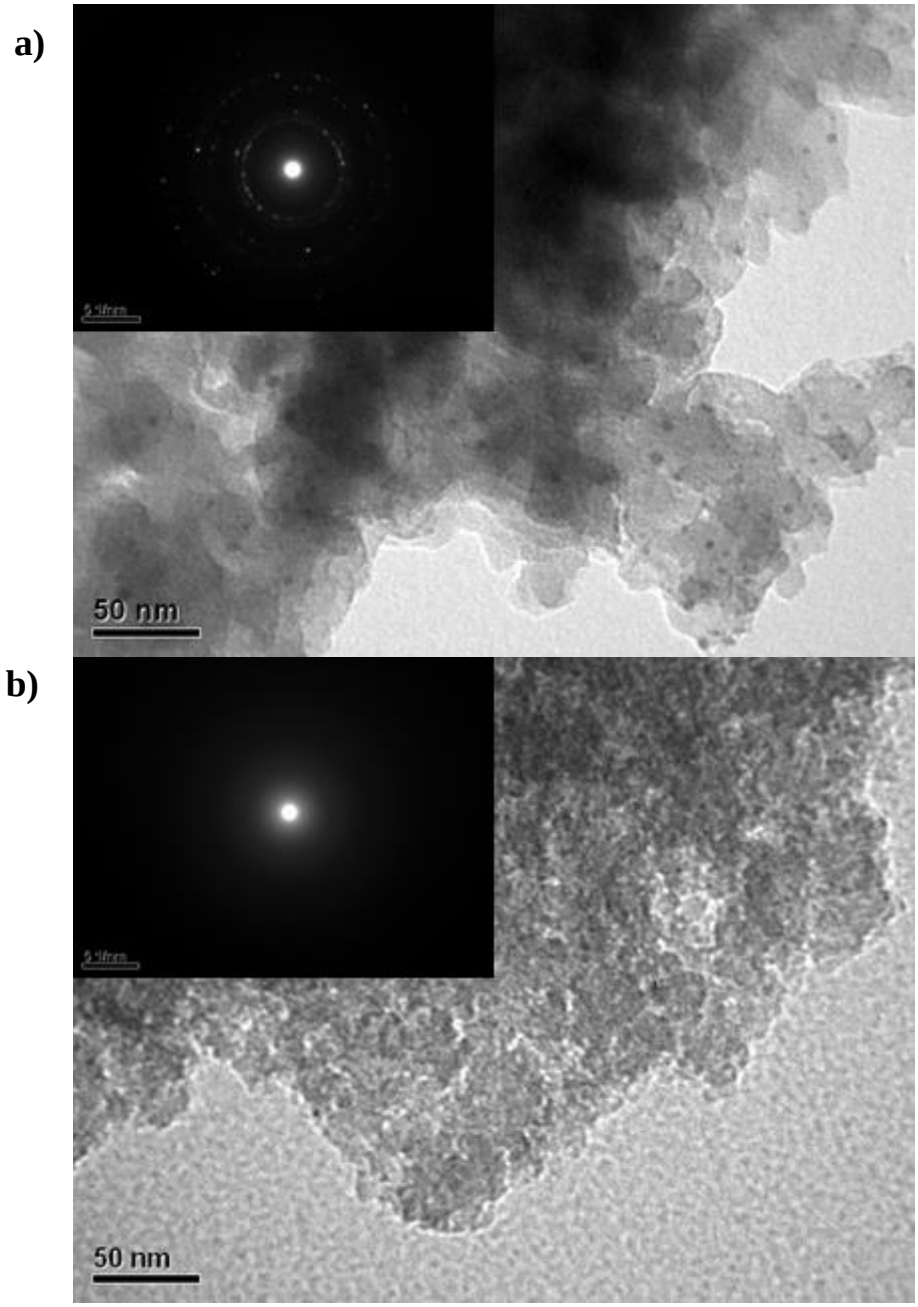

Figure 10. TEM micrographies and electron diffraction analysis for the synthetized materials. a) PdAS(10)MS and b) PdAS(10)OS

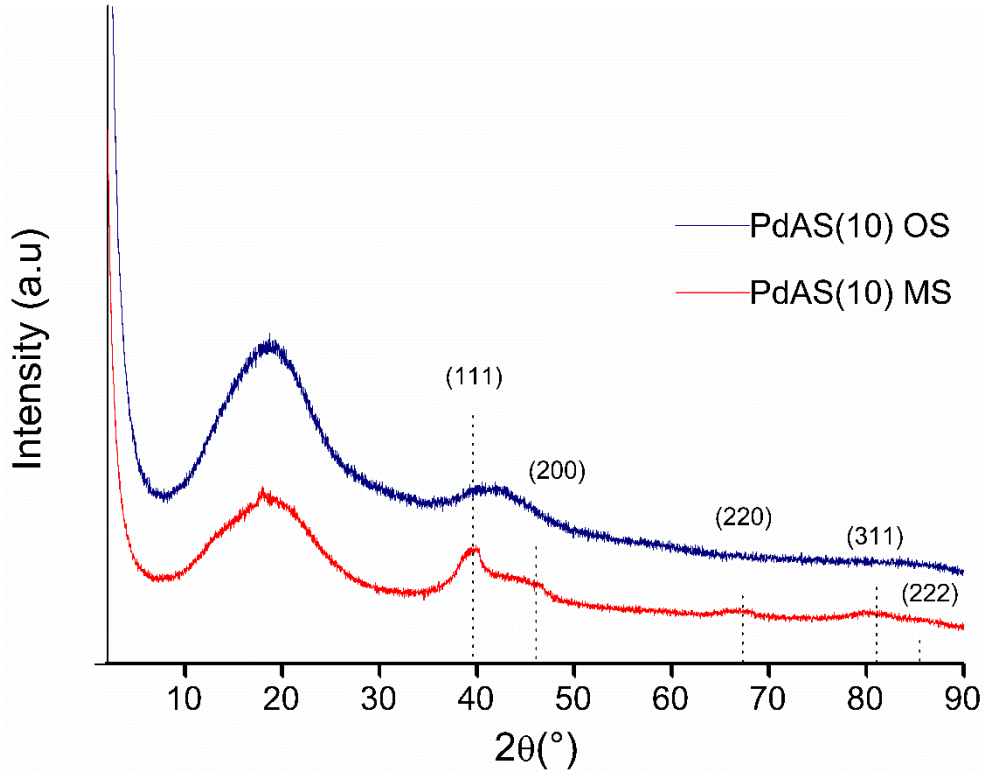

Figure 11. XRD analysis for the syntethized materials.

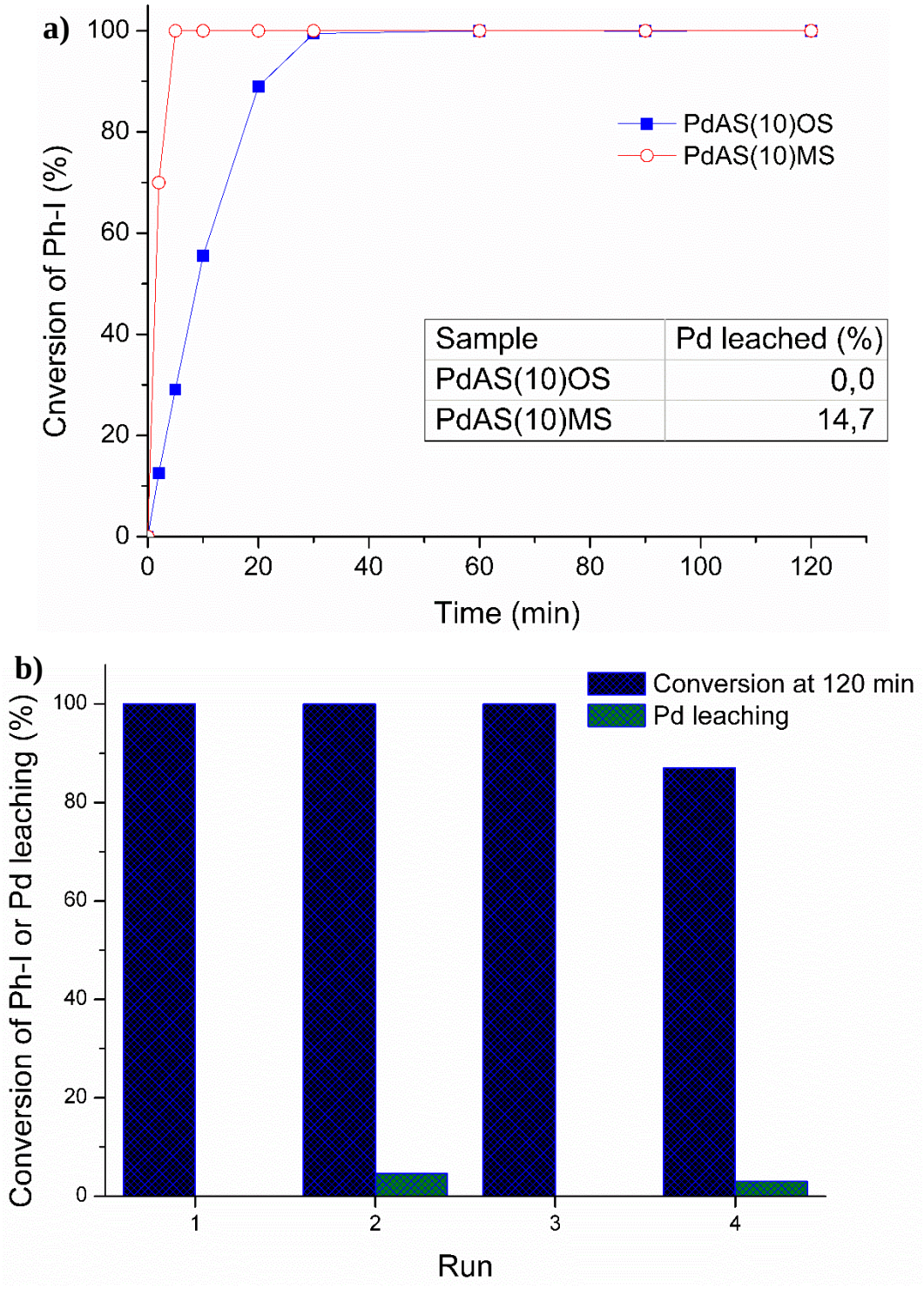

Figure 12. a) Catalytic evaluation of PdAS(10)MS and PdAS(10)OS in Heck coupling of IB and MA and leaching test determined by ICP-OES (inset table). b) Recycle study for PdAS(10)OS catalyst in Heck reaction of IB and MA.

Table 1. Organic Elemental Analysis of AS ligand and Pd-AS free complex.

Sample	% C_{exp}	% C_{theo}	% H_{exp}	% H_{theo}	% N_{exp}	% N_{theo}
AS	78.73	78.76	5.92	6.10	7.28	7.07
Pd-AS	60.29	62.35	3.92	4.43	6.11	5.59

Table 2. Textural properties of AS(10), PdAS(10)MS and PdAS(10)OS.resins.

Resin	$S_{B.E.T}$ (m^2g^{-1})	Pore volume (cm^3g^{-1})	Pore size (nm)
AS(10)	705	0.95	12
PdAS(10)MS	713	0.96	13
PdAS(10)OS	754	1.314	22

Table 3. Comparison of PdAS(10)OS performance in MA-IB heck reaction with literature reports.

Catalyst	Temperature °C	Conversion (%)	Reusability (cycles)	TOF (h^{-1})	Ref
Pd onto magnetic dendritic polymer (Fe_3O_4@SiO_2-Dendrimer-Pd)	120	96	5	16000	[62]
Pd^{II} immobilized onto PVA-modified hydrogel (Pd^{II} nanosheet)	140	100	6	13889	[63]
Pd-imidazolium complex immobilized on polystyrene polymer (Pd(II)-POLI-TAG)	130	>99	5	487	[64]
Pd Salen complex onto Polystyrene polymer (PS-Pd-Salen)	110	79	5	138	[65]
PdAS(10)OS	120	100	4	6122	This work

Table 4. Catalytic evaluation of PdAS(10)OS resins

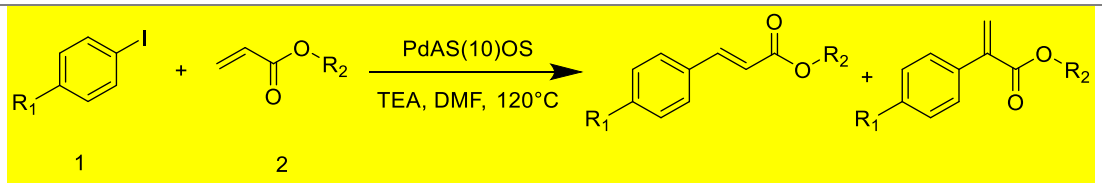

Entry	Reactant 1	Reactant 2	Conversion*	Product
1	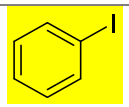	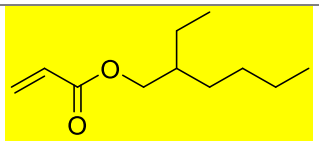	100	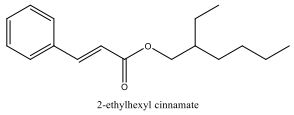 2-ethylhexyl cinnamate
2	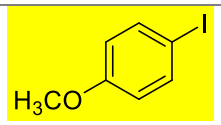	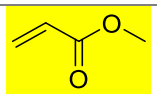	100	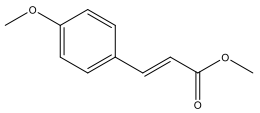 methyl (*E*)-3-(4-methoxyphenyl)acrylate
3	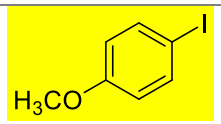	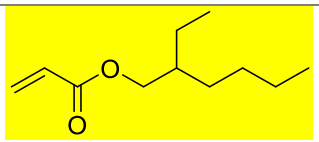	100	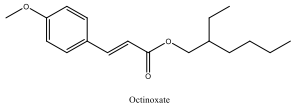 Octinoxate
4	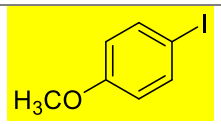	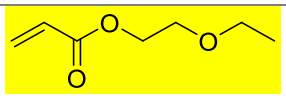	100	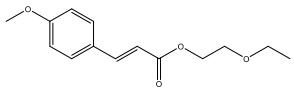 Cinoxate

* Conversion based on the disappearance of Iodoarene at 60 minutes of reaction.

Table of Content

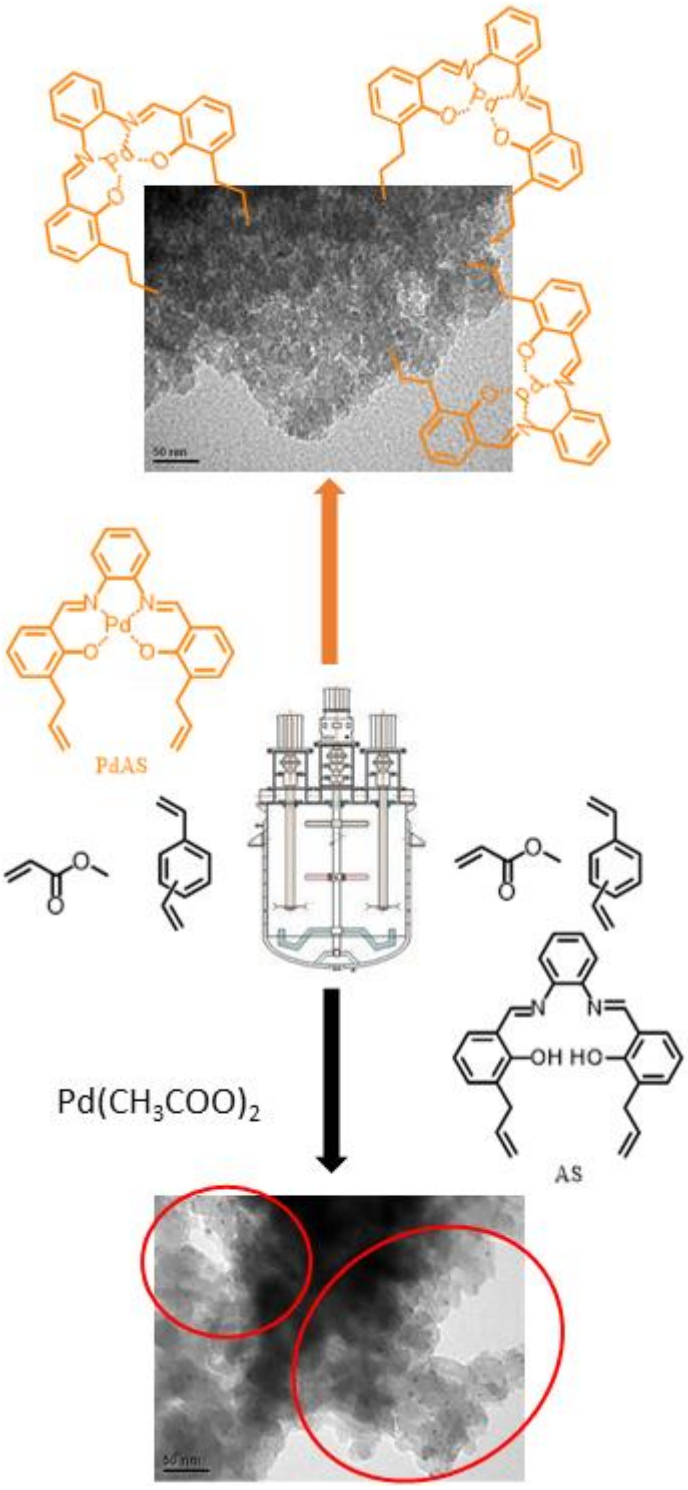

Two polymerization route was evaluated, to obtain a immobilized palladium coordination compounds, but only one, the "one-step" synthetic route, by polymerization of MCM is suitable to obtain the immobilized coordination compound.

6. References.

1. Corma, A., and Garcia, H., *Advanced Synthesis & Catalysis* (2006) **348** (12-13), 1391
2. Shaikh, I. R., *Journal of Catalysts* (2014) **2014**, 402860
3. Martínez, A., *et al.*, *Catalysis Science & Technology* (2015) **5** (1), 310
4. Pálinkó, I., Heterogeneous Catalysis: A Fundamental Pillar of Sustainable Synthesis. (2018)
5. Sheldon, R. A., *Green Chemistry* (2017) **19** (1), 18
6. Beletskaya, I. P., and Kustov, L. M., *Russian Chemical Reviews (Print)* (2010) **79** (6), 441
7. Anastas, P. T., *et al.*, *Applied Catalysis A: General* (2001) **221** (1), 3
8. Zarnegaryan, A., *et al.*, *Journal of the Iranian Chemical Society* (2019) **16** (4), 747
9. Balas, M., *et al.*, *European Journal of Inorganic Chemistry* (2021) **2021** (16), 1581
10. Veerakumar, P., *et al.*, *ACS Sustainable Chemistry & Engineering* (2017) **5** (8), 6357
11. Zhao, X. S., *et al.*, *Materials Today* (2006) **9** (3), 32
12. Jadhav, S., *et al.*, *Transition Metal Chemistry* (2019) **44** (6), 507
13. Dewaele, A., *et al.*, *Catalysis Science & Technology* (2016) **6** (8), 2580
14. Nuri, A., *et al.*, *ChemistrySelect* (2019) **4** (5), 1820
15. Bharathi, M., *et al.*, *Journal of Porous Materials* (2019) **26** (5), 1377
16. Nikoorazm, M., *et al.*, *Applied Organometallic Chemistry* (2018) **32** (4), e4282
17. Vibhute, S. P., *et al.*, *Tetrahedron Letters* (2020) **61** (17), 151801
18. Nuri, A., *et al.*, *Catalysis Letters* (2020) **150** (9), 2617
19. Alamgholiloo, H., *et al.*, *Applied Organometallic Chemistry* (2018) **32** (11), e4539
20. Dhakshinamoorthy, A., *et al.*, *Chemical Society Reviews* (2015) **44** (7), 1922
21. Soorholtz, M., *et al.*, *ACS Catalysis* (2016) **6** (4), 2332
22. Altava, B., *et al.*, *Chemical Society Reviews* (2018) **47** (8), 2722
23. Anwander, R., Immobilization of Molecular Catalysts. In *Handbook of Heterogeneous Catalysis*, pp 583
24. Dong, K., *et al.*, *Catalysis Science & Technology* (2017) **7** (5), 1028
25. Maria Michela, D., *et al.*, *Current Organic Chemistry* (2013) **17** (12), 1236
26. Dzhardimalieva, G. I., *et al.*, *Journal of Inorganic and Organometallic Polymers* (2002) **12** (1), 1
27. Pomogailo, A. D., *Macromolecular Symposia* (1998) **131** (1), 115
28. Dey, T. K., *et al.*, *New Journal of Chemistry* (2018) **42** (11), 9168
29. Campos, C. H., *et al.*, *RSC Advances* (2017) **7** (6), 3398
30. Albéniz, A. C., and Carrera, N., *European Journal of Inorganic Chemistry* (2011) **2011** (15), 2347
31. Leadbeater, N. E., and Marco, M., *Chemical Reviews* (2002) **102** (10), 3217
32. Xia, L., *et al.*, *ChemistryOpen* (2019) **8** (1), 45
33. Jadhav, S. N., *et al.*, *New Journal of Chemistry* (2015) **39** (3), 2333
34. Boruah, J. J., *et al.*, *Green Chemistry* (2013) **15** (10), 2944
35. Cai, Y., *et al.*, *Journal of Applied Polymer Science* (2019) **136** (3), 46979
36. Mohamed, M. H., and Wilson, L. D., *Nanomaterials (Basel)* (2012) **2** (2), 163
37. Santora, B. P., *et al.*, *Macromolecules* (2001) **34** (3), 658
38. Niakan, M., *et al.*, *Colloids and Surfaces A: Physicochemical and Engineering Aspects* (2018) **551**, 117
39. Hamasaka, G., *et al.*, *Advanced Synthesis & Catalysis* (2018) **360** (9), 1833
40. Jagtap, S., *Catalysts* (2017) **7** (9), 267
41. Nasrollahzadeh, M., *et al.*, *Molecular Catalysis* (2020) **480**, 110645
42. Alexander, S., *et al.*, *Journal of Molecular Catalysis A: Chemical* (2009) **314** (1), 21
43. Hassan, H. M. A., *et al.*, *Applied Catalysis A: General* (2014) **488**, 148

44. Basu, P., *et al.*, *Journal of Organometallic Chemistry* (2018) **877**, 37
45. Layek, S., *et al.*, *Journal of Organometallic Chemistry* (2017) **846**, 105
46. Sobhani, S., *et al.*, *Catalysis Letters* (2016) **146** (1), 255
47. Nikoorazm, M., *et al.*, *Journal of Porous Materials* (2016) **23** (4), 967
48. Das, P., and Linert, W., *Coordination Chemistry Reviews* (2016) **311**, 1
49. Sardarian, A. R., *et al.*, *Dalton Transactions* (2019) **48** (9), 3132
50. He, F. F., *et al.*, *Journal of Radioanalytical and Nuclear Chemistry* (2013) **295** (1), 167
51. Wei, J., *et al.*, *Journal of Applied Polymer Science* (2004) **92** (4), 2681
52. Mota, V. Z., *et al.*, *Spectrochimica Acta Part A: Molecular and Biomolecular Spectroscopy* (2012) **99**, 110
53. Choudhary, A., *et al.*, *ACS Omega* (2017) **2** (10), 6636
54. Kumari, S., *et al.*, *Inorganic Chemistry* (2019) **58** (2), 1527
55. Li, Y., *et al.*, *Polymer Degradation and Stability* (2001) **73** (1), 163
56. More, S., *et al.*, *Molecular Catalysis* (2017) **442**, 126
57. Zhu, X. X., *et al.*, *Macromolecules* (1999) **32** (2), 277
58. Celebioglu, A., *et al.*, *New Journal of Chemistry* (2019) **43** (7), 3146
59. Eswaran, M., *et al.*, *Fuel* (2019) **251**, 91
60. Li, Y., *et al.*, *Journal of Applied Polymer Science* (2015) **132** (1)
61. Amini, M., *et al.*, *RSC Advances* (2012) **2** (32), 12091
62. Ma, R., *et al.*, *New Journal of Chemistry* (2018) **42** (6), 4748
63. Nagai, D., *et al.*, *ACS Omega* (2020) **5** (29), 18484
64. Mahmoudi, H., *et al.*, *Green Chemistry* (2019) **21** (2), 355
65. Balinge, K. R., and Bhagat, P. R., *Inorganica Chimica Acta* (2019) **495**, 119017

WILEY-VCH

Immobilized Pd metal-complex on polymeric resin with high surface areas for recyclable catalyst: Effect of the immobilization method on nature of palladium species.

Claudio Mella[1*], *Gina Pecchi*[1,2], *Cyril Godard*[3], *Carmen Claver*[3], *Abdiel Márquez*[4], *Javiera Herrera*[1],*Cristian H Campos*[1]

[1]Facultad de Ciencias Químicas, Universidad de Concepción, Casilla Concepción 160-C, Chile,

[2]Millenium Nuclei on Catalytic Processes towards Sustainable Chemistry (CSC), Chile,

[3]Departmento de Química Física e Inorgánica, Universitat Rovira i Virgili, Tarragona, España.

[4]Centro de Nanociencias y Nanotecnología, Universidad Nacional Autónoma de México, Ensenada Baja California, México.

Correspondence to Claudio Mella, Postdoctoral research of Polymer Department, Universidad de Concepción, Casilla Concepción 160-C, Chile. E-mail: claudiomella@udec.cl

Keywords: Immobilization; synthetic route; palladium complex; metal-containing monomer.

Abstract

A critical query on literature is the approach used to immobilize homogeneous catalysts to improve their efficiency and recyclability. This work aims to compare the immobilization level of a kind of Pd-N,N'-bis(salicylidene)-o-phenylenediamine complex on high surfaces of polymeric resins to provide heterogenous catalysts for Mizorocki-Heck reaction. The preparation method involves two strategies: i) polymerization of the ligand before the complex-synthesis in a "multi-step (MS)" approach and ii) a direct "one-step" (OS) immobilization by polymerization of the metal-containing monomers (MCMs) as co-monomer. Both approaches effectively yield polymers with a larger surface area, over 700 m^2g^{-1}, and suitable thermic properties to use in the proposed reaction. In addition, the characterization of the polymers by XRD, XPS, and TEM demonstrates notable differences in Pd species on polymer support associated with the methodological approach to immobilizing the metal complex.

1. Introduction

The immobilization of metal coordination compounds has become essential for obtaining pseudo-homogeneous catalysts [1-3]. These catalysts take advantage of the excellent catalytic properties in terms of activity and selectivity of the homogeneous catalysts, with easy separation from the reaction medium and reusability [4-7]. Among different strategies for immobilization, covalent bonding is the most used methodology to obtain a stable, recoverable, and reusable immobilized coordination catalyst [**8,9**]. In this way, two different approaches have been established for the covalent immobilization of coordination compounds[10,11], as detailed in schematic 1. The first one (A) is called “multi-step synthesis” (MS), where the active phase is synthesized step by step until to obtain a surface-immobilized coordination compound, while the second one (B) is called “one-pot synthesis” (OS) when the immobilization of the coordination complex is produced in situ.

Different inorganic and organic solids have been used to immobilize coordination compounds, such as SiO_2 [1,12-16], and Fe_3O_4 particles[17,18] , among others. Commonly, these inorganic matrixes needed surface grafting with linkers molecules to provide a covalent anchoring point for the immobilization of coordination compounds, which are generally focused on the MS approach. This approach presents a competitive effect between the adsorption of the metal precursor into the solid and metal coordinated by ligands on the surface. On the other hand, organic materials applied to metal coordination compound immobilization can be represented for metal-organic frameworks [18-20] and polymeric materials as covalent triazine frameworks[21], dendrimers, and polystyrene-based resins, as has been reviewed by Altava et al.[22]. Polymer matrixes are attractive materials to try the OS approach, especially using self-immobilization of metal-containing monomers (MCMs)[23-27], to keep control over the molecular structure of the metal coordination compound. Within the polymeric materials, the synthetic resin based on styrene (Sty) and divinylbenzene co-polymers [28-31], especially the commercial Merrifield resins[32-34], stand up for immobilization of coordination compounds due to its excellent thermal and mechanical properties. Additionally, Merrifield resins can be easily chemical modified; nonetheless, polymeric resin presents a drawback related to its limited surface area, which could result in a restrictive property to the accessibility[29] of the reactants to the active site, limiting their catalytic efficiency. Fortunately, the suspension polymerization methodology using is a facile and economic methodology to obtain polymeric resins with a large surface area and controlled porosity [35-37].

Pd-based catalysts play a significant role in different organic reactions, acting as one of the essential organic synthesis tools. Therefore, many works have reported immobilized Pd-coordination compounds [16,38-41]. Especially, Pd Schiff-bases metal complexes are employed as homogeneous catalysts in different reactions such as hydrogenation[42], epoxidation[43], carbonylation[44] and carbon cross-coupling[38,45-49], because there are highly stable and cheaper

than typical Pd-phosphine complexes. Therefore, it is essential to develop the most suitable approach for immobilizing coordination compounds over polymeric matrixes to enhance their catalytic applications.

This work aims to synthesize and characterize immobilized pseudo-homogeneous catalysts into polymers with high surface area and their catalytic performance for the Mizorocki-Heck reaction. We propose that two methodological synthesis routes effectively obtain the Pd Schiff-base immobilized into surfaces of polymers with high surface area. We also report the textural, thermal, and spectroscopy evidence about coordination complexes immobilization and Pd-species. Finally, both materials were tested in the C-C coupling reaction to prepare cinnamic methyl ester starting from the methyl acrylate and iodobenzene at optimized reaction conditions.

2. Materials and Methods

2.1. *Materials*

Sodium chloride, palladium (II) acetate $Pd(CH_3COO)_2$, ethanol absolute (EtOH), n-hexane, iodobenzene (IB), and acetone (99.5%) were purchased from Merck®. Hydroxyethyl-cellulose (HEC, 99%, ~90000 MW), 3-allylsalicylaldehyde (97%), o-phenylenediamine (99.5%), and divinylbenzene (DVB, technical grade 80%) were purchased from Sigma Aldrich®. Methyl acrylate (MA, 99% Aldrich®) was distilled at normal pressure in the presence of p-tert-butylcatechol as an inhibitor; 2,2'-azobisisobutyronitrile (AIBN, Aldrich®) was purified by recrystallization from methanol; dichloromethane (DCM, 99% Merck®) was dried with CaH_2; toluene (≥ 99.0% Merck®) was dried over Na(s) and distilled previously to use.

2.2 Characterization techniques

Chemical analysis of the samples was conducted by inductively coupled plasma optical emission spectrometry (ICP-OES) using a Spectro Arcos instrument. The preparation of the samples included an HNO_3 and H_2SO_4 microwave acid treatment on a Milestone Srl model Ethos Easy and then diluted for further analysis.

Thermogravimetric analysis (TGA) was performed at a heating rate of 10°min-1 up to 900°C with N_2 flow of 8.0 mL/min in NETZSCH TG instrument model 209F1 Iris, using 3.0 mg of sample.

The ^{13}C decoupling, ^{1}H NMR, C-H correlation NMR, and solid-state ^{13}C CP-MAS NMRs analysis were performed on a Mercury VX400 VARIAN.

Nitrogen adsorption isotherms at a temperature of -196°C were obtained on a Micromeritics apparatus Model TriStar II Series 2; the specific area was calculated using the B.E.T method, while the pore size distribution and pore volume by BJH method.

SEM and TEM characterized the morphology of the samples; the first one was on an SEM-Probe CAMECA model SU-30 coupled to an EDS probe, and the second was on a Jeol JEM-1200 EXII. Gaussian distribution analysis of the diameter of 600 particles was used to estimate the average particle diameter.

A Bruker FT-IR model Vertex 70 was used for FT-IR analysis. A Thermo Scientific Bio UV-Vis Spectrophotometer model Evolution 260 was used for UV-VIS spectroscopy analysis.

Elemental analysis of AS ligand and Pd-AS metallo-monomer were characterized on a Sartorius balance model M2P and Perkin Elmer Elemental analyzer model EA2400.

XPS measurements were performed using a VG Escalab 200R electron spectrometer equipped with a hemispherical electron analyzer and Mg Kα (1253.6 eV) as the X-ray source.

Lastly, XRD patterns were obtained with nickel-filtered CuKa1 radiation (λ=1.5418 Å) on a Rigaku diffractometer and collected from the range of 20-90° for 2Θ.

2.3 Synthesis of AS and PdAS.

Schematic 2 shows the AS ligand and PdAS MCM synthesis route. A typical synthesis involves the dissolution of 40.0 mmol of 3-allylsalicylaldehyde on EtOH mixed with a dissolution of 20.0 mmol o-phenylenediamine in 50 mL of EtOH refluxed for two hours. Then, the mixture was cooled, and the resultant solid was recrystallized from EtOH to obtain the orange solid ligand AS[50]. For PdAS MCM synthesis, the AS ligand was dissolved in a solution of dichloromethane and $Pd(CH_3COO)_2$, using a 1:1 ratio between Pd and AS. The mixture was kept under stir for 12 hours to obtain a brown solid, washed after, and recrystallized on the DCM/n-hexane mixture.

2.4 Synthesis of PdAS(10) MS and PdAS(10) OS resins.

The literature suggests that the resin synthesis must be in a three-neck polymerization reactor [29,51]. The synthesis involved 60, 29, 10, and 1 wt.% of DVB, MA, AS (or PdAS), and AIBN:

1. The co-monomers and initiator were mixed and stirred for 10 min.
2. Toluene was added to the mixture and kept for 10 min under stirring.
3. The mixture was suspended over an aqueous phase in a three-neck polymerization reactor (containing 20 wt.% of NaCl and 0.2 wt.% of HEC) at 400 rpm mechanical stirring.

The polymerization was carried out at 70°C for 14 hours and 88°C for 4 hours under N_2 flow (10 mL·min^{-1}).

.For MS methodology, the yellow polymer beads were washed with water and acetone for 48 hours in a Soxhlet extractor and dried at 83°C in a vacuum oven. Materials were denominated AS(10) resin. AS(10) resin was contacted with an excess of $Pd(CH_3COO)_2$ solution in DCM (with 1:1.1 nominal molar ratio AS on polymeric materials in $Pd(CH_3COO)_2$ for 12h, washed with DCM, and dried on a vacuum oven overnight, to obtain brown PdAS(10)MS resin.

With the OS approach, brown beads of PdAS(10)OS resin were obtained by self-polymerization of PdAS and washed in a Soxhlet extractor with water and DCM. Then, the acquired resin PdAS(10)OS beads were dried at 83°C in a vacuum oven.}

2.5 Catalytic evaluation.

The catalytic Heck coupling reaction of IB and MA was evaluated as a test reaction, and the most promising catalyst was evaluated in the recycle test. In a typical reaction, 50 mg of catalyst was dissolved on specific precursors based on the desired amount of Pd. The reactant conditions were IB:Pd 2000:1 and IB:MA:TEA 1:1.25:2. The reaction was carried out in a Parr-type semi-batch reactor at 120°C in Ar (5.5 bar), at 770 rpm of magnetic stirring, using 50mL of DMF as solvent, and dodecane as the internal standard. The catalytic activity was measured at different times.

The samples were taken over 1 mL of water, followed by extraction with Et_2O (1000 µL) and washing with 1 mL of brine. The conversion was measured in terms of IB consumption, analyzing the organic layer at a Perkin Elmer GC model Clarus 680, equipped with an Elite-MS5 capillary column. Additionally, the leaching evaluation was carried out by analysis of the post-reaction catalytic mixture

3. Results and Discussion.

3.1. AS and PdAS characterization.

Pure AS ligand was obtained as an orange solid with 80% yield after recrystallization. The ^{1}H -^{13}C HSQC NMR spectra (400 MHz, $CDCl_3$, 25 °C) of the AS shown in Figure 1a confirms the AS structure with the characteristic peaks at 3.45, 5.06, 5.09, and 6.06 ppm related to allyl groups. The peaks between 6.86 to 7.34 ppm are associated with an aromatic structure. The protons peaks of imine and alcohol appear at 8.63 and 13.3 ppm, respectively, according to He *et al*[50]. The orange line in the FT-IR spectra in Figure 2a shows the expected band associated with hydroxile and imine distinct groups, corresponding to AS ligand at 3440 (-OH) and 1614 cm^{-1} (-C=N-) [50,52]. In addition, the orange line of UV-Vis spectra (DCM) shown signals at 229 and 278 nm related to typical $\pi \rightarrow \pi^*$ transition of aromatics ring and azomethine group and $n \rightarrow \pi^*$ transition at 341 nm.

In Figure 1b, the ^{1}H–^{13}C HSQC NMR spectra (400 MHz, $CDCl_3$, 25 °C) of PdAS demonstrate the obtention of PdAS MCM without decomposition of ligand, with the expected disappearance of the -OH signal. In the FT-IR spectra of the PdAS coordination compound, the black line in Figure 2a, the characteristic displacement of the wave number of imine band to 1602 cm^{-1} (-C=N-), and the disappearance of the signals related to OH confirmed the PdAS formation.

UV-Vis spectra (DCM) in Figure 2b show the signals of aromatic $\pi \rightarrow \pi^*$ transition band at 244 nm, $\pi \rightarrow \pi^*$ and $n \rightarrow \pi^*$ transition bands between 336 and 355 nm, with a bathochromic shift by metal center coordination, confirmed by the apparition of a new transition at 481 nm related with charge-transfer (C-T)/ d-d transition[53,54].

Figure 3 shows the wide XPS spectrum range, identifying the binding energies and auger emissions for the surface atomic components on the PdAS coordination complex. Only one surface Pd $3d_{5/2}$, at 339.60 eV, and a spin-orbital splitting of 5.27 eV for the $3d_{3/2}$ component was detected. This Pd surface specie was compared with the $Pd(CH_3COO)_2$ precursor that present BE at 338.4 eV for $3d_{5/2}$ and 343.7 for $3d_{3/2}$ core level.

The spectroscopy data confirms the formation of AS ligand and PdAS coordination compound with two polymerizable groups. In addition, the organic elemental analysis of AS and PdAS summarized in Table 1 confirms the expected chemical formula.

3.2 AS(10), PdAS(10) MS and PdAS(10) OS resins characterization

Figure 4 demonstrates the N_2 adsorption-desorption isotherms of the PdAS(10)OS, PdAS(10)MS immobilized Pd polymers, and the AS(10)resin. All materials exhibited isotherm with narrow hysteresis loop at high pressure, classified as type IV on IUPAC classification, characteristic of mesoporous materials or interstitial spaces in agglomerates of nanoparticles. Table 2 displays the surface areas over 700 m^2g^{-1}. AS(10) resin did not show significant changes in textural properties after contact with $Pd(CH_3COO)_2$ on both resin precursor and PdAS(10)MS; with pore diameter near 13 nm and a minimal increase in the surface area related to a more surface exposed in broken material.

On the other hand, PdAS (10)OS resin showed a significant increase in surface area and mean pore diameter. The differences in pore diameter can be related to a different monomer mixture's solubility on single drop-in presences or absences of metallic center coordinated directly on an AS monomer[36].

TGA measure for the immobilized polymers presents high decomposition temperature, as shown in the thermal decomposition profile in Figure 5. This elevated decomposition

temperature is associated with the high crosslinked grade of synthesized polymers with T_{50} at 451 and 442°C for PdAS(10)OS and PdAS(10)MS resins, respectively[55].

SEM micrographs for AS(10) resin in Figure 6a picture the expected spherical morphology for a typical suspension polymerization process. By Gaussian distribution (inset of Figure 6a) was possible estimated an average diameter value of 216 µm.

This regular morphology for crosslinker resin was broken entirely after contact with $Pd(CH_3COO)_2$ to form PdAS(10)MS resin, as shown in Figure 6b. A similar result has been previously reported for Jadhav for an immobilized Pd catalyst prepared by M.S approach, pass from well-defined microparticles to powder kind material[33,56]. Additionally, the surface EDS techniques in Figure 7 showed obtaining 0.5% Pd to broken PdAS(10)MS resin and 1.2% Pd to spherical PdAS(10)OS resin, respectively. ICP-OES measured similar trends in Pd loading, with 0.7 wt.% for PdAS(10)MS and 1.4 wt.% for PdAS(10)OS. These values indicate that the OS approach immobilizes twice the Pd amount compared to the MS methodology.

Figure 8a displays the solid ^{13}C CP-MAS NMR spectra for PdAS(10)MS and PdAS(10)OS. The principal signals are related to the DVB[57] main component that masks the principal signals of the coordination compound in the aromatic zone and the central polymer backbone at 33 ppm, as well as the methyl moieties of ethylbenzene technical grade DVB. In addition, it is possible to distinguish two signals attributed to the MA component in the polymer, the first one as a shoulder at 58 ppm related with $–OCH_3$ moiety and the second one of the carbonyl group at 184 ppm.

FTIR spectra in Figure 8b show the same evidence; the influential absorption bands of C=O mask the Pd Schiff Base immobilized signal at 1739 cm^{-1} and C-O tension at 1164 cm^{-1} characteristic of MA, and the signals of aromatic vibrations of the

polymer. The only band associated with the Schiff-Base complex appears at 796 cm^{-1}, with no clear evidence to confirm the nature of Pd in the immobilized polymers. These are notable differences from others immobilized palladium complexes reported in the literature that FTIR analysis can identify.

The XPS analysis shed light on the chemical environment of surface palladium species in the PdAS(10) resins and has a comparison point concerning the PdAS-free complex. Figure 9a shows the Pd 3d spectra of the PdAS(10)MS and Figure 9b for PdAS(10)OS polymers. The spectra of Pd 3d for PdAS(10)OS fits a Pd $3d_{5/2}$ at 339.40 eV and Spin-orbital splitting at 5.3 eV, denoting one Pd oxidative state. Conversely, in the PdAS(10)MS, the deconvolution indicates at least two Pd oxidative states, the first at 336.1 eV typically attributed to the Pd^0 component and the second at 338.1 eV related to the Pd^{2+} component associated with $Pd(CH_3COO)_2$ precursor BE[58]. This mixture of Pd species can be understood due to the long-time of reaction and an impossibility to proceed to the metal complexation reaction, producing a reduction of $Pd(CH_3COO)_2$ precursor, similar to the effect for the same metallic precursor and comparative polymer matrix was reported previously by Mathew [59]. Therefore, the OS approach allowed the synthesis of the PdAS complex immobilized on polymers with high surface areas.

TEM characterization results reinforced the differences between MS and OS approaches. It is possible to see nanoparticles on the polymer surface for PdAS(10)MS in Figure 10a. Additionally, the electron diffraction pattern (inset of Figure 10a) was measured, obtaining the *d*-spacing values of 0.224; 0.193; 0.137, and 0.112 nm, coinciding to (111), (200), (220), (311) and (222) planes of palladium nanoparticles. Unlike PdAS(10)MS, PdAS(10)OS did not show metal particles on the surface or a diffraction pattern in electron diffraction analysis. The XRD analysis in Figure 11 exhibits the typical broad signals associated with the non-crystalline structure of crosslinked polymer matrix at 19° 2θ value[60] and a second shoulder around 43° 2θ

value. Furthermore, for PdAS(10)MS is possible to see the planes of diffraction associated with metallic Pd according to TEM characterization and XPS spectra.

3.3 Catalytic evaluation.

Both catalysts showed high catalytic performance of iodobenzene and methyl acrylate coupling reaction in Figure 12a. The PdAS(10)MS completed the reaction in 5 min, while the PdAS(10)OS catalyst showed a progressive conversion that reached 99% of conversion at 30 min. The leaching analysis can be related to the $Pd(CH_3COO)_2$ not immobilized on PdAS(10)MS, which can be leached to the reaction mixture and act as a homogeneous catalyst.

In counterpart, the PdAS(10)OS resin was confirmed to act as a heterogeneous catalyst after consecutive catalytic cycles, keeping the complete conversion of reactants as shown in Figure 12b with negligible minor Pd leached for the run. However, after the fourth cycle, the total leaching was 6% of the original Pd amount.

4. Conclusion.

This work provides solid evidence about the differences in the synthesis approach used to immobilize the PdAS complex in a polymeric resin with a high surface area. Different characterization techniques discarded our thesis of obtaining the same catalytic specie by different synthesis routes. The leaching test and possible reuse of PdAS(10)OS resin in consecutive catalytic cycles demonstrates the differences in the supported species in the polymer surface and their impact on catalytic performance.

Moreover, we can ratify that self-polymerization is the most efficient approach to immobilizing PdAS MCM, avoiding the metal nanoparticle aggregation and the leaching process in catalytic tests. Ultimately, the polymeric resin obtained by self-polymerization

exhibits superior performance in consecutive cycles of the Heck coupling reaction, capable of standing up to four cycles.

5. Acknowledgement.

In memory of Professor José Luis Garcia Fierrro. The authors would like to thank J.L.G. Fierro for his contribution to this work, and specifically his significant contribution to the XPS field. The authors thank to CESMI, Universidad de Concepción, for microscopy and NMR analysis. C.Mella acknowledges support from ANID FONDECYT 3200379; G. Pecchi acknowledges support from ANID FONDECYT 1210142.

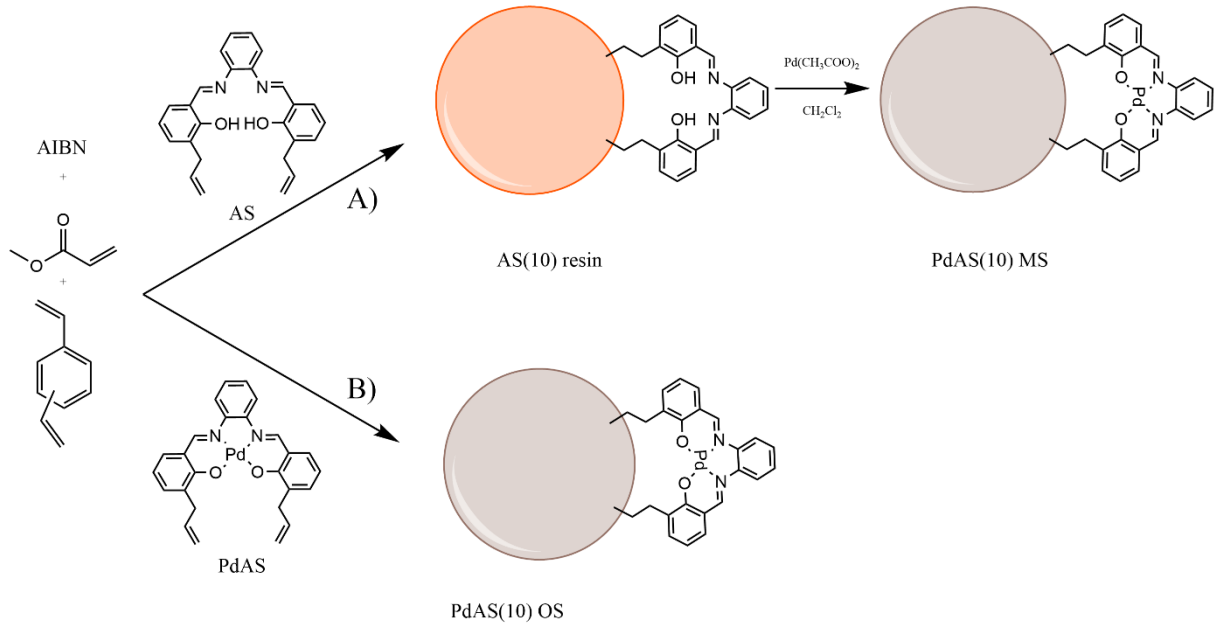

Scheme 1. Synthesis route evaluated to PdAS complex immobilization on polymeric resins.

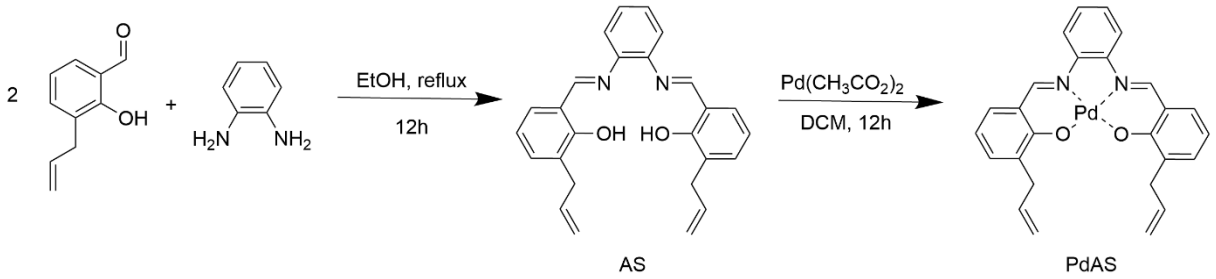

Scheme 2. AS and PdAS synthesis route.

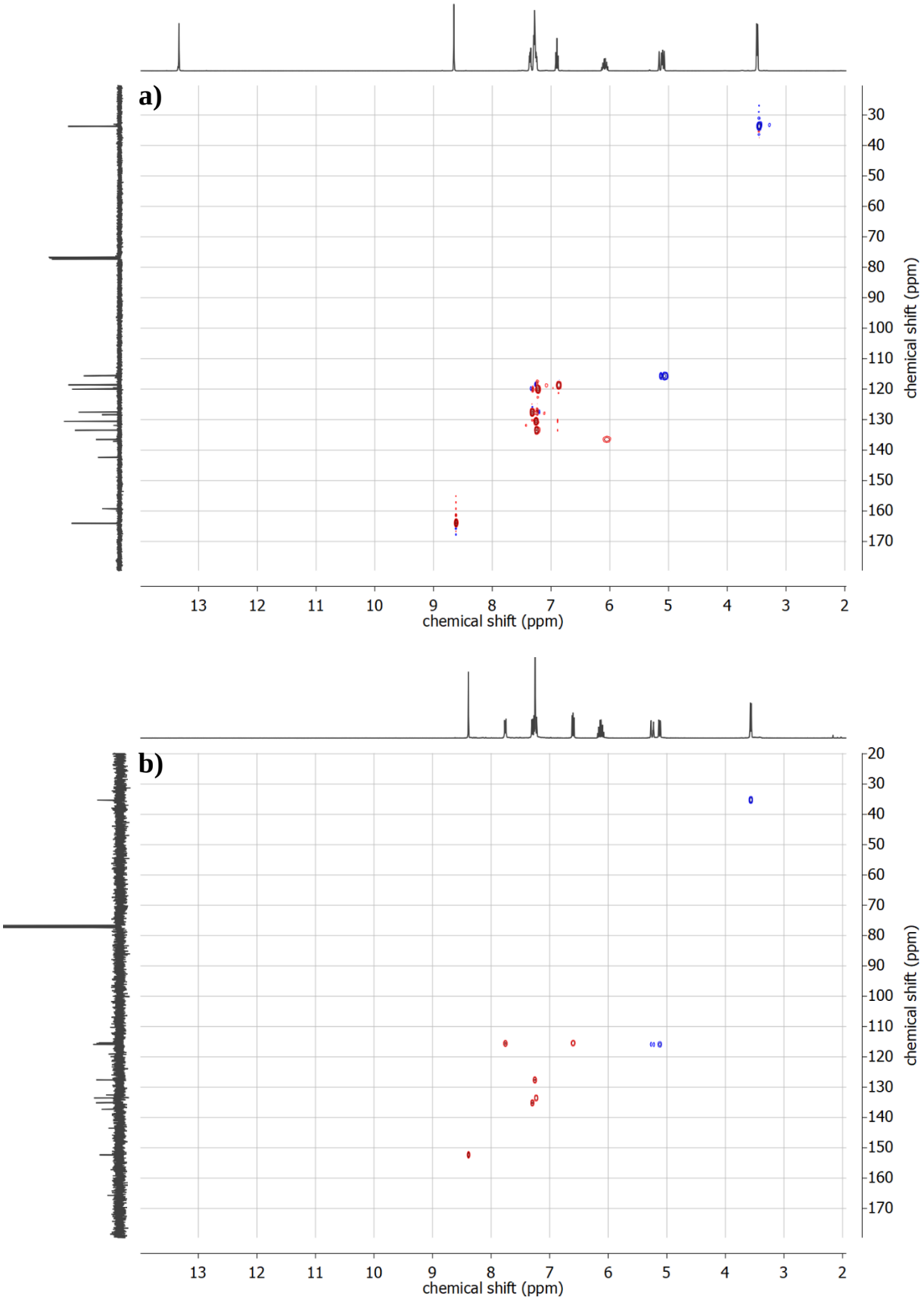

Figure 1. ^{1}H-^{13}C HSQC of a) AS ligand and b) PdAS MCM.

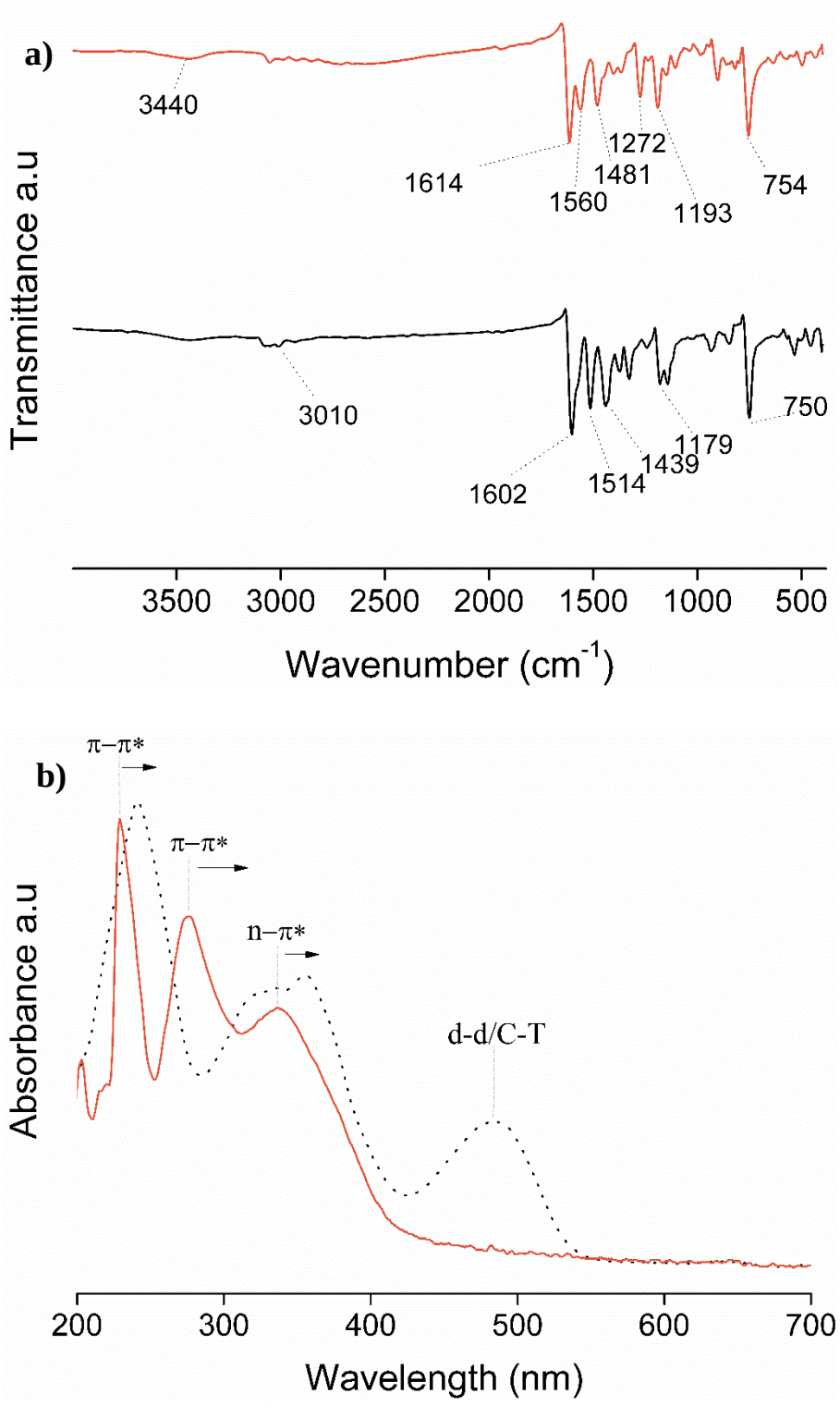

Figure 2. Spectroscopy characterization of AS free ligand and PdAS MCM by. a) FTIR Spectra in KBr pellet. b) UV-Vis spectra on CH_2Cl_2.

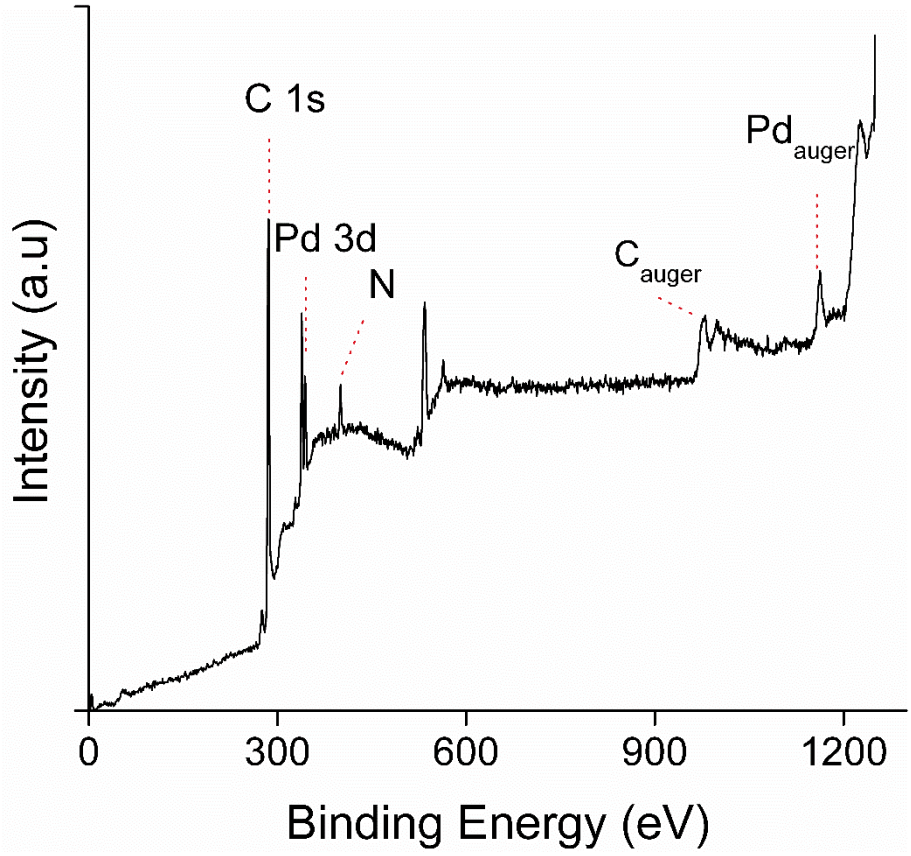

Figure 3. XPS spectra of PdAS free coordination complex.

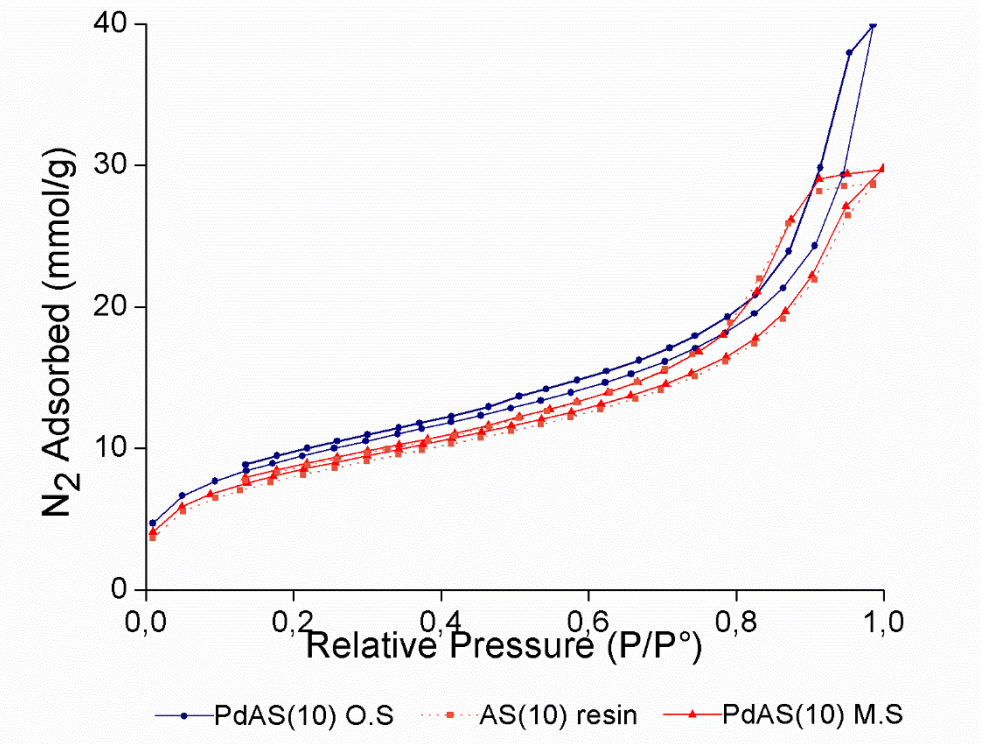

Figure 4. N_2 adsorption-desorption at -196°C isotherms for synthesized materials.

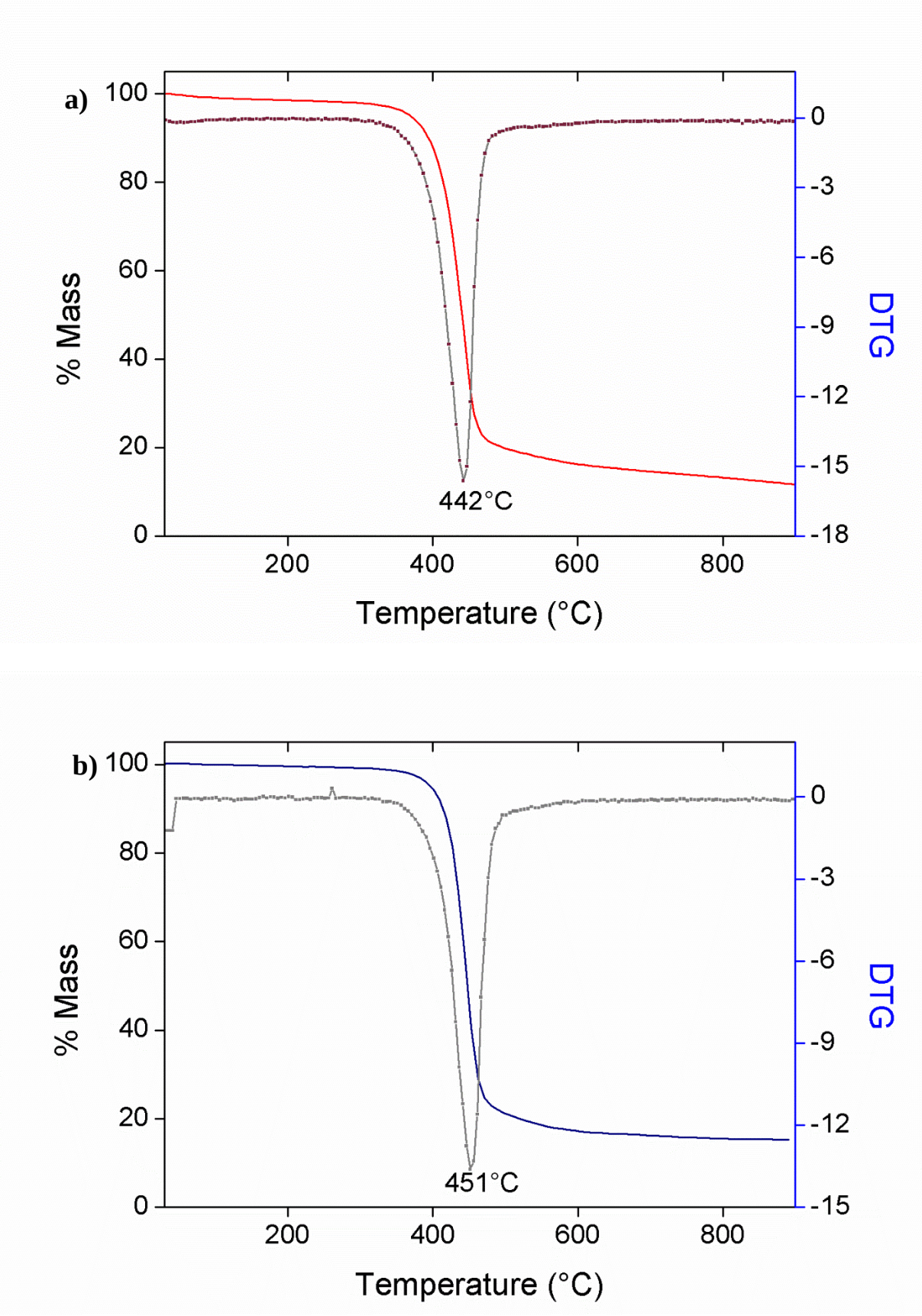

Figure 5. Thermogravimetric profile for (a) PdAS(10)MS (b) PdAS(10)OS.

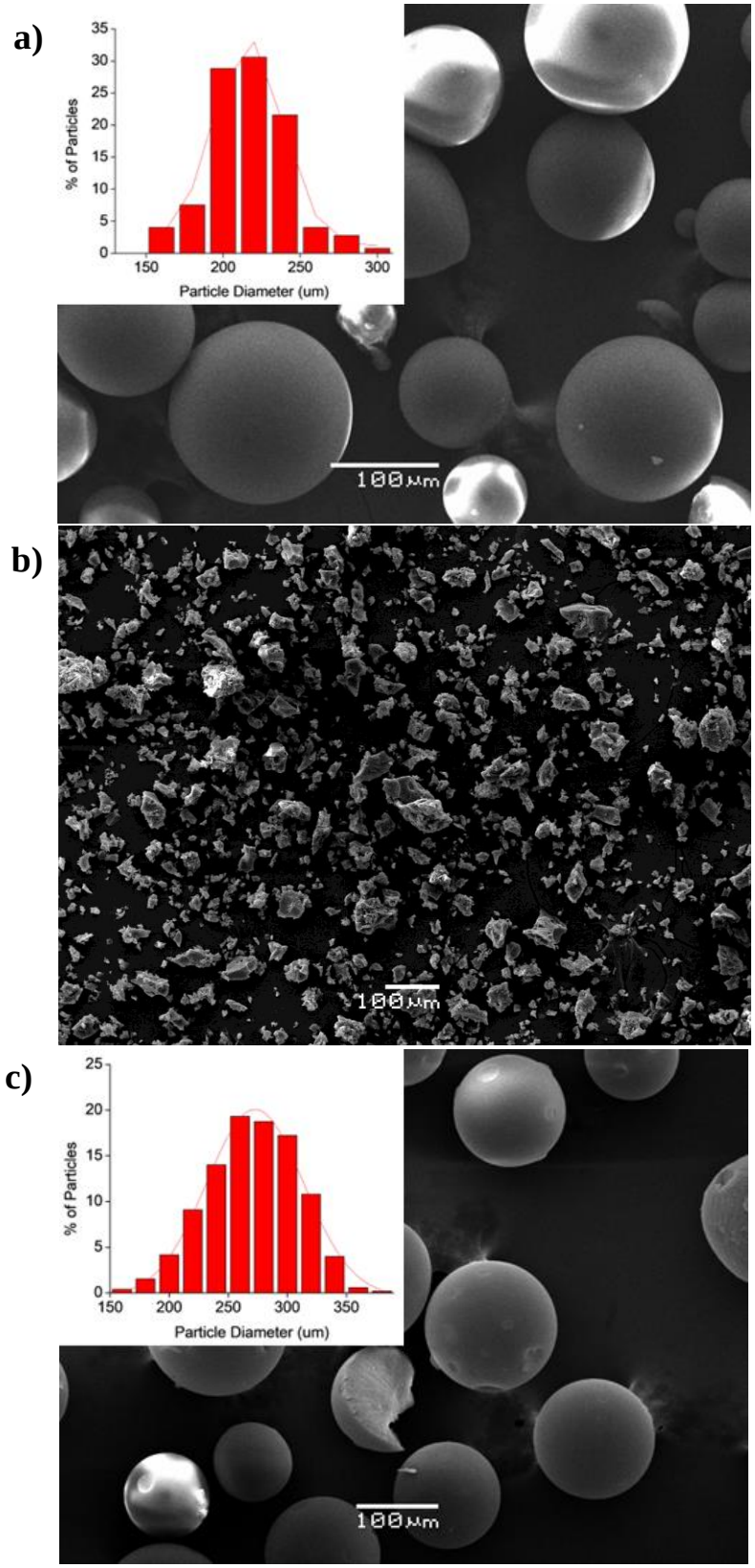

Figure 6. SEM micrographs for synthesized materials (a)AS(10) resin (b)PdAS(10)MS (c)PdAS(10)OS.

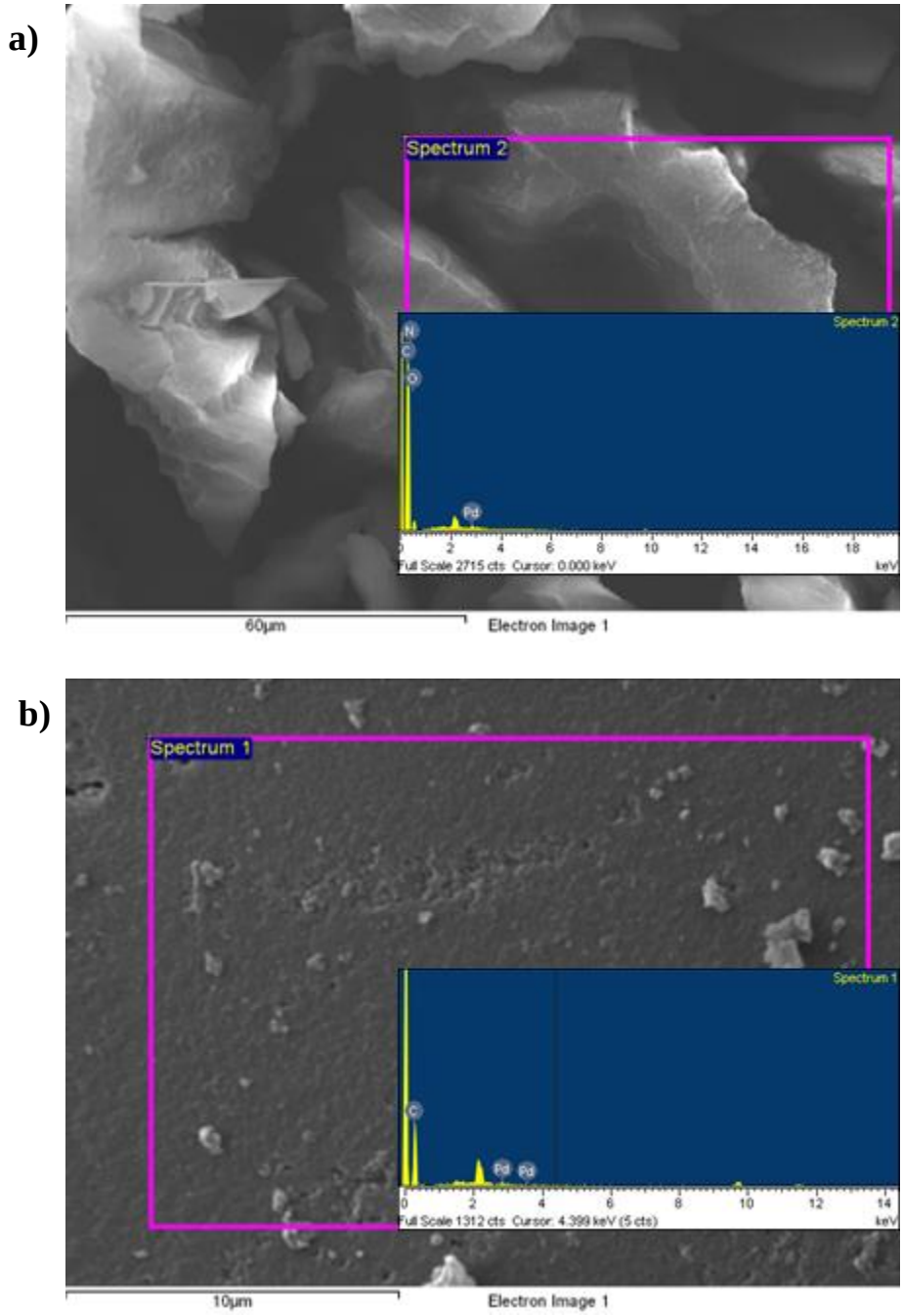

Figure 7. EDS analysis from SEM micrographs for synthesized materials (a)PdAS(10)MS and (b)PdAS(10)OS.

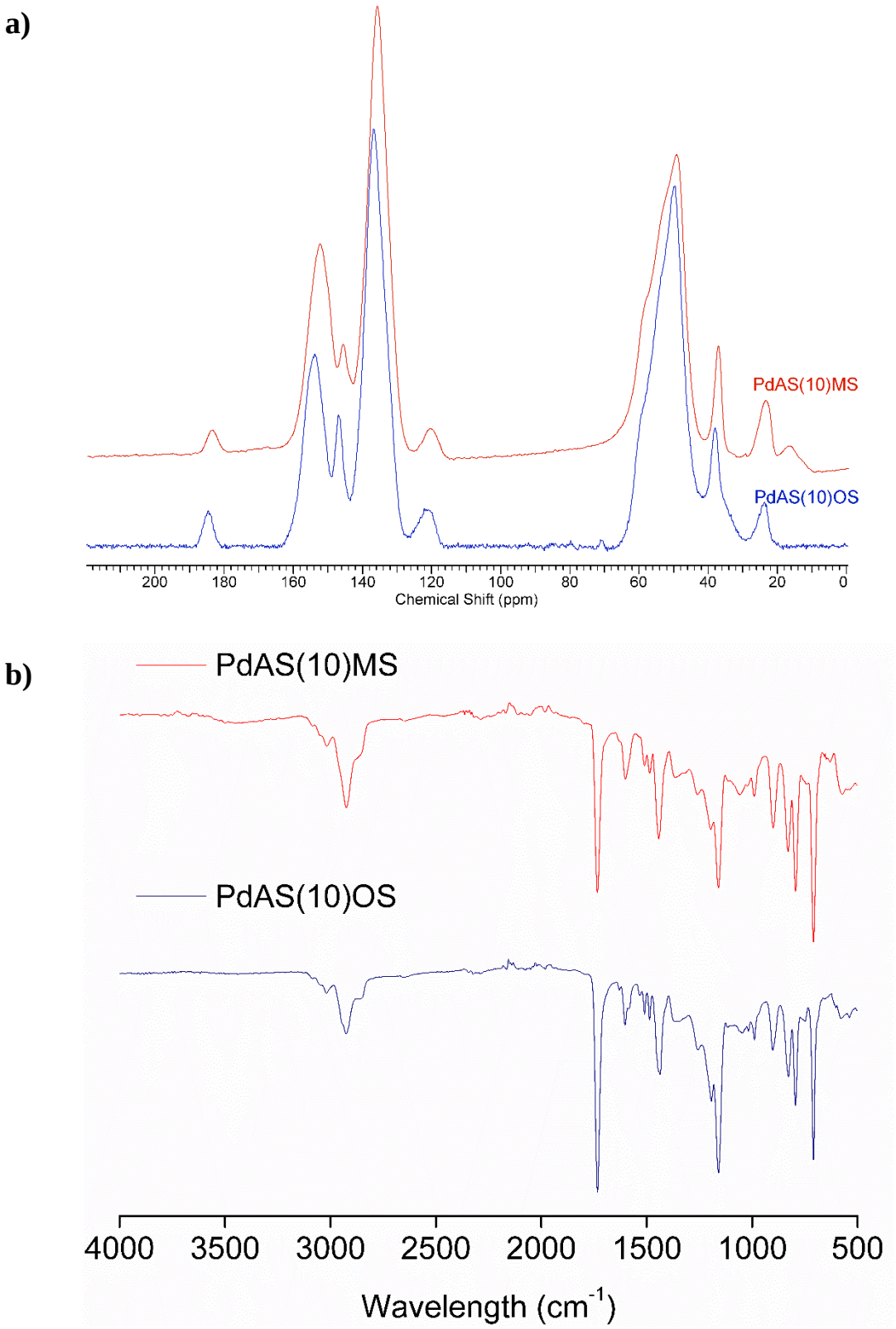

Figure 8. Spectroscopy characterization of PdAS(10)MS and PdAS(10)OS by (a)^{13}C-CP MAS NMR (b)FTIR.

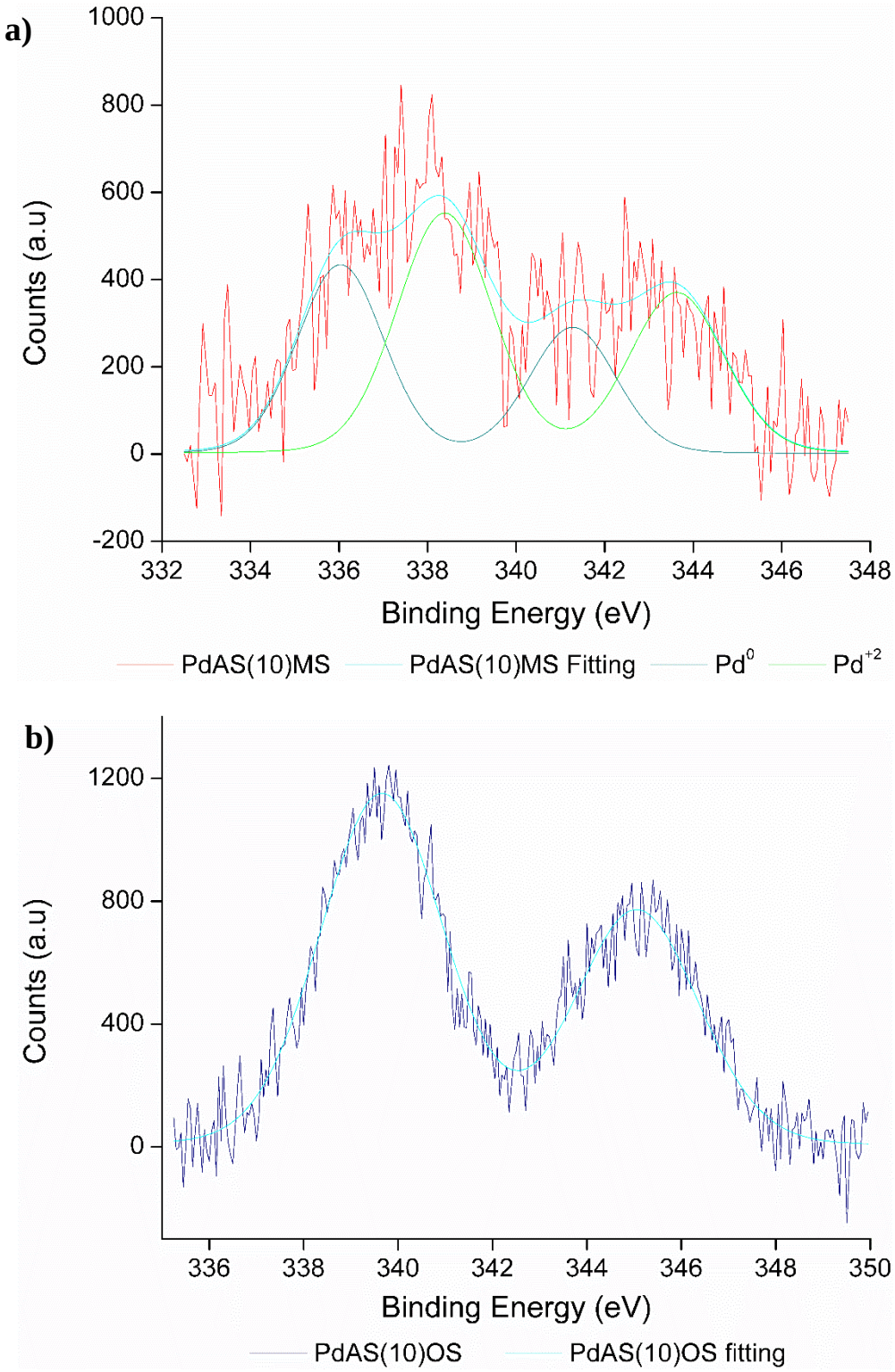

Figure 9. Spectroscopy XPS analysis a)PdAS(10)MS. b)PdAS(10)OS.

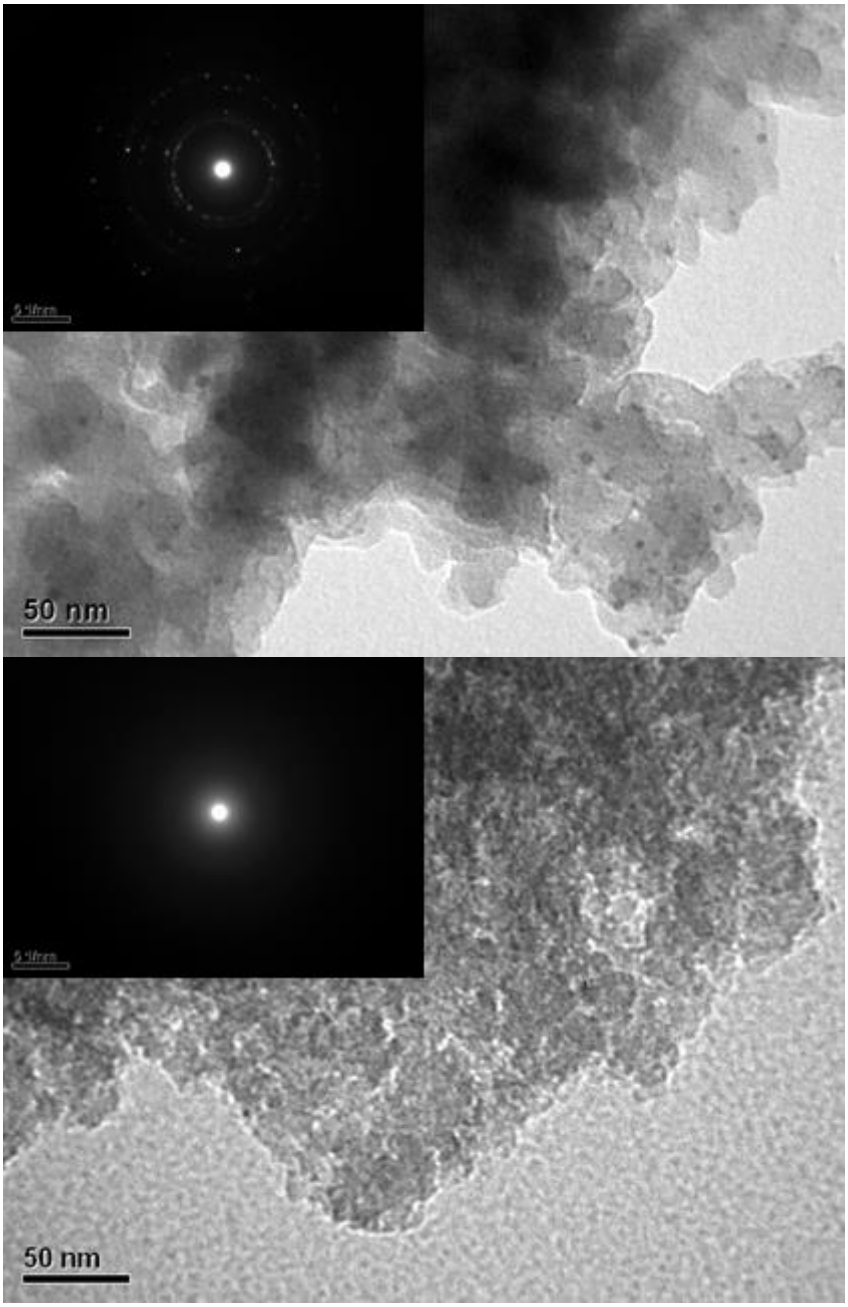

Figure 10. a) TEM micrography of PdAS(10)MS. b) TEM micrography of PdAS(10)OS

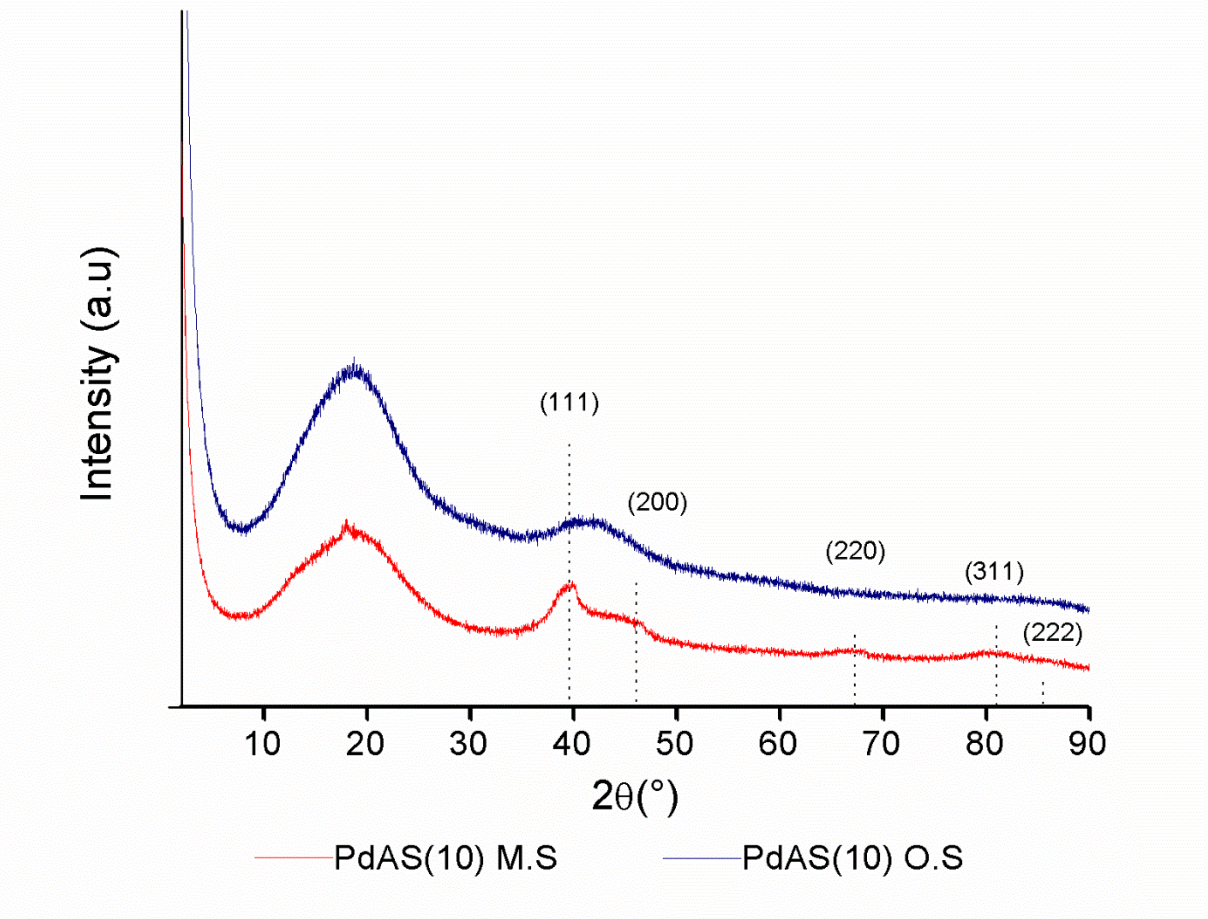

Figure 11. XRD analysis of PdAS(10)MS and PdAS(10)OS resins.

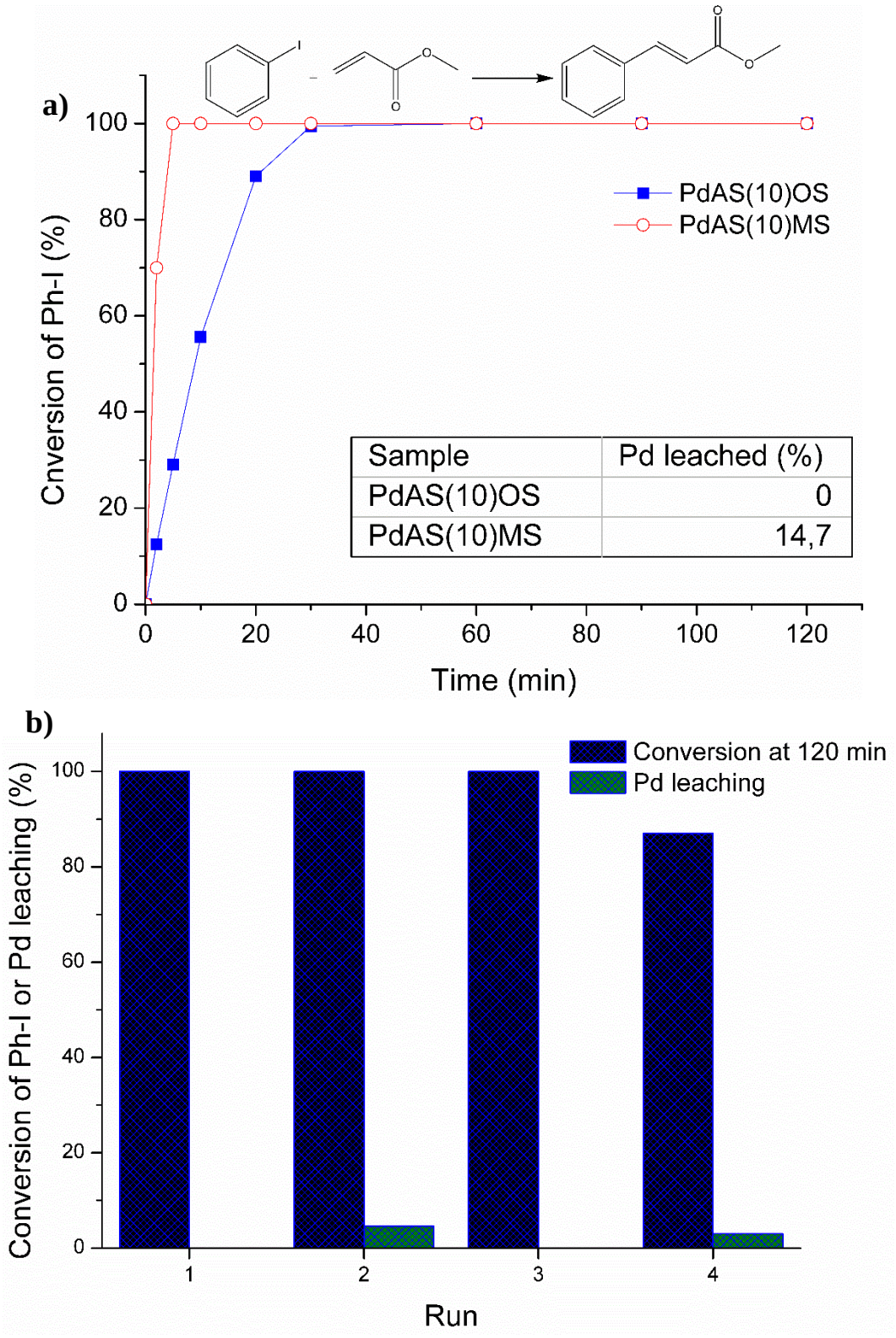

Figure 12. a) Catalytic evaluation of PdAS(10)MS and PdAS(10)OS in Heck coupling of iodobenzene and methyl acrylate and leaching test (inset). b) Recycle study for PdAS(10)OS catalyst in Heck reaction of IB and MA.

Table 1. Organic Elemental Analysis of AS ligand and Pd-AS free complex.

Sample	% C_{exp}	% C_{theo}	% H_{exp}	% H_{theo}	% N_{exp}	% N_{theo}
AS	78.73	78.76	5.92	6.10	7.28	7.07
Pd-AS	60.29	62.35	3.92	4.43	6.11	5.59

Table 2. Textural properties of AS(10), PdAS(10)MS and PdAS(10)OS.resins.

Resin	$S_{B.E.T}$ (m^2g^{-1})	Pore volume (cm^3g^{-1})	Pore size (nm)
AS(10)	705	0.95	12
PdAS(10)MS	713	0.96	13
PdAS(10)OS	754	1.314	22

Table of Content

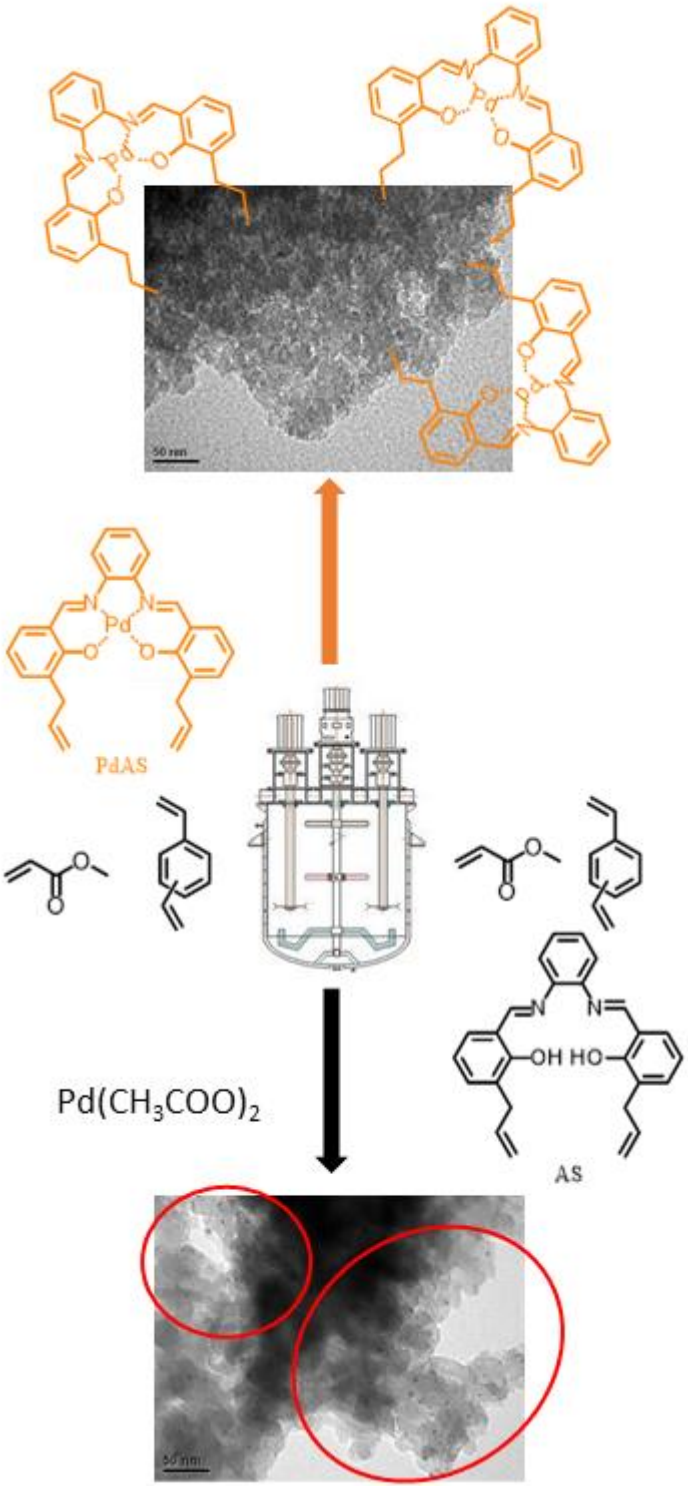

Two polymerization route was evaluated, to obtain a immobilized palladium coordination compounds, but only one, the "one-step" synthetic route, by polymerization of MCM is suitable to obtain the immobilized coordination compound.

6. References.

1. Corma, A., and Garcia, H., *Advanced Synthesis & Catalysis* (2006) **348** (12-13), 1391
2. Shaikh, I. R., *Journal of Catalysts* (2014) **2014**, 402860
3. Martínez, A., *et al.*, *Catalysis Science & Technology* (2015) **5** (1), 310
4. Pálinkó, I., Heterogeneous Catalysis: A Fundamental Pillar of Sustainable Synthesis. (2018)
5. Sheldon, R. A., *Green Chemistry* (2017) **19** (1), 18
6. Beletskaya, I. P., and Kustov, L. M., *Russian Chemical Reviews (Print)* (2010) **79** (6), 441
7. Anastas, P. T., *et al.*, *Applied Catalysis A: General* (2001) **221** (1), 3
8. Zarnegaryan, A., *et al.*, *Journal of the Iranian Chemical Society* (2019) **16** (4), 747
9. Balas, M., *et al.*, *European Journal of Inorganic Chemistry* (2021) **2021** (16), 1581
10. Veerakumar, P., *et al.*, *ACS Sustainable Chemistry & Engineering* (2017) **5** (8), 6357
11. Zhao, X. S., *et al.*, *Materials Today* (2006) **9** (3), 32
12. Jadhav, S., *et al.*, *Transition Metal Chemistry* (2019) **44** (6), 507
13. Dewaele, A., *et al.*, *Catalysis Science & Technology* (2016) **6** (8), 2580
14. Nuri, A., *et al.*, *ChemistrySelect* (2019) **4** (5), 1820
15. Bharathi, M., *et al.*, *Journal of Porous Materials* (2019) **26** (5), 1377
16. Nikoorazm, M., *et al.*, *Applied Organometallic Chemistry* (2018) **32** (4), e4282
17. Vibhute, S. P., *et al.*, *Tetrahedron Letters* (2020) **61** (17), 151801
18. Nuri, A., *et al.*, *Catalysis Letters* (2020) **150** (9), 2617
19. Alamgholiloo, H., *et al.*, *Applied Organometallic Chemistry* (2018) **32** (11), e4539
20. Dhakshinamoorthy, A., *et al.*, *Chemical Society Reviews* (2015) **44** (7), 1922
21. Soorholtz, M., *et al.*, *ACS Catalysis* (2016) **6** (4), 2332
22. Altava, B., *et al.*, *Chemical Society Reviews* (2018) **47** (8), 2722
23. Anwander, R., Immobilization of Molecular Catalysts. In *Handbook of Heterogeneous Catalysis*, pp 583
24. Dong, K., *et al.*, *Catalysis Science & Technology* (2017) **7** (5), 1028
25. Maria Michela, D., *et al.*, *Current Organic Chemistry* (2013) **17** (12), 1236
26. Dzhardimalieva, G. I., *et al.*, *Journal of Inorganic and Organometallic Polymers* (2002) **12** (1), 1
27. Pomogailo, A. D., *Macromolecular Symposia* (1998) **131** (1), 115
28. Dey, T. K., *et al.*, *New Journal of Chemistry* (2018) **42** (11), 9168
29. Campos, C. H., *et al.*, *RSC Advances* (2017) **7** (6), 3398
30. Albéniz, A. C., and Carrera, N., *European Journal of Inorganic Chemistry* (2011) **2011** (15), 2347
31. Leadbeater, N. E., and Marco, M., *Chemical Reviews* (2002) **102** (10), 3217
32. Xia, L., *et al.*, *ChemistryOpen* (2019) **8** (1), 45
33. Jadhav, S. N., *et al.*, *New Journal of Chemistry* (2015) **39** (3), 2333
34. Boruah, J. J., *et al.*, *Green Chemistry* (2013) **15** (10), 2944
35. Cai, Y., *et al.*, *Journal of Applied Polymer Science* (2019) **136** (3), 46979
36. Mohamed, M. H., and Wilson, L. D., *Nanomaterials (Basel)* (2012) **2** (2), 163
37. Santora, B. P., *et al.*, *Macromolecules* (2001) **34** (3), 658
38. Niakan, M., *et al.*, *Colloids and Surfaces A: Physicochemical and Engineering Aspects* (2018) **551**, 117
39. Hamasaka, G., *et al.*, *Advanced Synthesis & Catalysis* (2018) **360** (9), 1833
40. Jagtap, S., *Catalysts* (2017) **7** (9), 267
41. Nasrollahzadeh, M., *et al.*, *Molecular Catalysis* (2020) **480**, 110645
42. Alexander, S., *et al.*, *Journal of Molecular Catalysis A: Chemical* (2009) **314** (1), 21
43. Hassan, H. M. A., *et al.*, *Applied Catalysis A: General* (2014) **488**, 148

44. Basu, P., *et al.*, *Journal of Organometallic Chemistry* (2018) **877**, 37
45. Layek, S., *et al.*, *Journal of Organometallic Chemistry* (2017) **846**, 105
46. Sobhani, S., *et al.*, *Catalysis Letters* (2016) **146** (1), 255
47. Nikoorazm, M., *et al.*, *Journal of Porous Materials* (2016) **23** (4), 967
48. Das, P., and Linert, W., *Coordination Chemistry Reviews* (2016) **311**, 1
49. Sardarian, A. R., *et al.*, *Dalton Transactions* (2019) **48** (9), 3132
50. He, F. F., *et al.*, *Journal of Radioanalytical and Nuclear Chemistry* (2013) **295** (1), 167
51. Wei, J., *et al.*, *Journal of Applied Polymer Science* (2004) **92** (4), 2681
52. Mota, V. Z., *et al.*, *Spectrochimica Acta Part A: Molecular and Biomolecular Spectroscopy* (2012) **99**, 110
53. Choudhary, A., *et al.*, *ACS Omega* (2017) **2** (10), 6636
54. Kumari, S., *et al.*, *Inorganic Chemistry* (2019) **58** (2), 1527
55. Li, Y., *et al.*, *Polymer Degradation and Stability* (2001) **73** (1), 163
56. More, S., *et al.*, *Molecular Catalysis* (2017) **442**, 126
57. Zhu, X. X., *et al.*, *Macromolecules* (1999) **32** (2), 277
58. Celebioglu, A., *et al.*, *New Journal of Chemistry* (2019) **43** (7), 3146
59. Eswaran, M., *et al.*, *Fuel* (2019) **251**, 91
60. Li, Y., *et al.*, *Journal of Applied Polymer Science* (2015) **132** (1)

Graphical Abstract Image